Universiteit Utrecht

Institute for Theoretical Physics

Master Thesis

Holographic QCD at non-zero Density under an External Magnetic Field

Author:
Alexandros Aerakis BSc

Supervisor:
dr. Umut Gürsoy

A thesis submitted in partial fulfilment of the requirements for the degree of Master of Science

August 2014

Abstract

We study, based on the AdS/CFT correspondence, the effects of non-zero charge density Q and external magnetic field B on large N_c QCD-like theories at finite temperature via two gravity duals. The first one is the Kraus-D'Hoker model, a $5D$ Einstein-Maxwell supergravity truncation dual to $\mathcal{N} = 4$ super-Yang-Mills theory in $3 + 1$ dimensions. We find that at large magnetic field the near-horizon geometry is BTZ$\times\mathbb{R}_2$ exhibiting holographically the dimensional reduction happening in the field theory. We also study the response of Q to the applied B in the grand canonical ensemble and find that it increases giving hints on how charge renormalizes with magnetic field. The second theory is a bottom-up Veneziano QCD model with ratio of flavours over colors $\chi = \frac{N_f}{N_c} = \frac{1}{10}$. We give an heuristic calculation of how T_c increases with B and study the thermodynamics of the deconfined phase. Our results show that the free energy is a decreasing function of B while the entropy and charge density increase, as in the Kraus D'Hoker case.

Contents

Introduction **2**

1 Quantum Chromodynamics **4**
1.1 Brief Introduction to QCD 4
1.2 Lattice QCD 7

2 Quark-Gluon Plasma from Gauge/Gravity Duality **15**
2.0.1 The AdS/CFT Correspondence 15
2.0.2 The Holographic Dictionary 17
2.0.3 Generalizations 18
2.0.4 AdS/CFT Correspondence and QCD 20
2.0.5 Confinement 21
2.0.6 Fundamental Matter in AdS/CFT 23

3 AdS/QCD **27**

4 The Holographic Models **33**
4.1 The Kraus-D'Hoker Model 33
4.2 Veneziano QCD 37
4.2.1 The Background 39
4.2.2 Thermodynamics 41

Discussion and Outlook **46**

Acknowledgements **48**

Appendices **49**
Appendix A: The Wilson-Loop Test 50
Appendix B: The A-coordinate System 51
Appendix C: Numerical Method 52

Introduction

Quantum Chromodynamics (QCD) is a very prolific ground for studying different phases of matter thanks to confinement and asymptotic freedom. At extreme conditions of high temperature and density, as realised in heavy-ion collisions, a new state of deconfined matter called the Quark-Gluon Plasma (QGP) forms for very short time and seems to behave as a very fluid with extremely small viscosity exhibiting thus strong coupling. Such collisions with non-vanishing impact parameter are also known to generate magnetic fields comparable to the strong interactions and can drive the system to novel phases, to new directions in the phase diagram, that can give a definite experimental signature. So, understanding how the magnetic field alters the dynamics can enrich the picture we have not only about Quantum Chromodynamics but also other systems, such as the Quantum Hall Effect.

The strong coupling of QCD up to the QGP phase does not allow for a perturbative treatment. In lack of exact non-perturbative tools, people so far have been using lattice simulations near equilibrium and hydrodynamic simulations to study non-equilibria phenomena. However, with the advent of the gauge/gravity duality correspondence, there was a boom of attempts to apply it to realisable strongly coupled systems such as QCD. Nowadays, AdS/CFT constitutes a fresh approach to these problems. The subject of this thesis is mainly the holographic description of Quantum Chromodynamics in the presence of a magnetic field.

In chapter 1, we give an overview of QCD physics and the predictions of lattice simulations with the recent results for QCD in external magnetic field. In Chapter 2, we formulate the gauge/gravity duality and motivate its application to QCD while in Chapter 3 we review relevant holographic models. In Chapter 4, we study two gravity theories. The first comes from supergravity and is dual to $\mathcal{N} = 4$ super-Yang-Mills theory. The second is more phenomenological and dual to cousins of QCD-like theories. There, we present our results on the thermodynamics and the effect of the magnetic field on them. Finally, we make concluding remarks and discuss the many possible extensions of this work.

1 | Quantum Chromodynamics

1.1 Brief Introduction to QCD

Quantum Chromodynamics is the well-established physical model describing the strong interactions between the constituents of the hadrons, quarks and gluons. It is a prototype of a Non-Abelian Quantum Field Theory with $SU(3)$ as the gauge group and gluons its associated gauge fields. The quarks transform in the fundamental representation of $SU(3)$ and appear in 6 types called flavors.

The Lagrangian of Quantum Chromodynamics reads

$$\mathcal{L}_{QCD} = \sum_{i=1}^{6} \bar{\psi}_i \big(i \not{D} - m \big) \psi_i - \frac{1}{4} G^a_{\mu\nu} G^{a\mu\nu}, \tag{1.1}$$

where $\psi_i(x)$ the quark field of flavor i and $G^a_{\mu\nu} = \partial_\mu A^a_\nu - \partial_\nu A^a_\mu + g f^{abc} A^b_\mu A^c_\nu$ is the field strength of the gauge field A^a_μ.

In contrast to Quantum Electrodynamics, QCD exhibits two peculiar features:

- At high energies, short distances, there is *Asymptotic Freedom*. This means that at high energies the coupling constant runs towards zero, rendering the quarks and gluons more and more weakly coupled. Counter-intuitive as it may seem, this weak coupling allows for very accurate perturbative calculations at deep inelastic scattering processes. These experiments provided the evidence that baryons and mesons have internal structure matching with what QCD proposed.

- At low energies, large distances, there is *Confinement*. As it turns out, the finite energy asymptotic states in QCD turn out to be color singlets we experimentally identify with the hadrons. Consequently, quarks and gluons cannot be observed individually and are said to be confined inside the hadrons. Towards low energies an energy scale Λ_{QCD} is generated below which the coupling is strong and perturbation theory

collapses. Thus, confinement is regarded a purely non-perturbative phenomenon. Although an analytic proof for this is missing, works on QCD on discretised spacetime (Lattice QCD) give hints of a flux tube of gauge fields forming between two quarks yielding a linear attractive potential confining them.

Besides the local $SU(3)$ symmetry, there is an important global symmetry in QCD in the case of massless quarks. That is the *chiral symmetry*. For instance, for only u and d massless quarks, the left-handed components are decoupled from the right-handed ones, therefore they can be transformed independently. That is a $U(2)_L \times U(2)_R$ symmetry

$$\begin{pmatrix} u \\ d \end{pmatrix}_L \to U_L \begin{pmatrix} u \\ d \end{pmatrix}_L, \ \begin{pmatrix} u \\ d \end{pmatrix}_R \to U_R \begin{pmatrix} u \\ d \end{pmatrix}_R,$$

which is decomposable to $SU(2)_{L+R} \times SU(2)_{L-R} \times U(1)_B \times U(1)_A$. The axial symmetry $U(1)_A$ is broken at the quantum level, $U(1)_B$ is the baryon number conservation and the diagonal $SU(2)_{L+R}$ corresponds to the isospin symmetry. The $SU(2)_{L-R}$ subgroup which rotates the left and right-handed particles in an opposite way is broken by the creation of quark-antiquark condensates in a manner similar to superconductivity. In particular, the chiral symmetry is spontaneously broken by a non-zero vacuum expectation value $\left\langle 0 \left| \bar{\psi}\psi \right| 0 \right\rangle = \left\langle 0 \left| \bar{\psi}_R\psi_L + \bar{\psi}_L\psi_R \right| 0 \right\rangle$ which mixes the helicities. Those 3 broken group generators give rise to 3 massless Goldstone bosons. However, in reality the quarks are massive and the chiral symmetry is not exact but explicitly broken. Nevertheless, the three lightest mesons, the pions, have the same quantum numbers as those Goldstone bosons and they satisfy the Gell-Mann-Oakes-Renner (GOR) relation

$$m_\pi^2 = \frac{(m_q + m_{\bar{q}})\sigma}{f_\pi^2},$$

where σ is the chiral condensate and f_π the pion's decay constant. Therefore, those mesons can be thought as by-products of a hidden chiral symmetry.
To conclude with, it should be stressed that the chiral symmetry breaking is another phase transition that is distinct and still interconnected with confinement.

The Quark-Gluon Plasma

At extreme temperatures and densities, well above the hadronic phase, it is considered that quarks and gluons are highly energetic and form what is

called *Quark-Gluon Plasma*. This should correspond to the phase of Big Bang just before hadronization, having then many implications on nucleosynthesis.

This state of matter is being investigated in heavy-ion collisions in RHIC and LHC. There, two opposite beams of Pb or Au nuclei collide at center-of-mass energies $\sqrt{s} \approx 200$ GeV/nucleon. During a central collision, a ball of QGP forms at the region of impact for 1 fm/c before it cools down and hadronizes. Initially, it was believed that this QGP phase is already in the weak coupling regime. Non-central collisions gave a different answer though. The QGP drop now is asymmetric with higher expansion pressure on its thin side (figure 1.1a). This anisotropy produces a non spherical distribution of hadrons (elliptic flow) at late times and yields information about the interactions in the plasma. Experiments showed that the shear viscosity η is the lowest measured in nature, indicating strong coupling (figure 1.1b). This is a remarkable manifestation of strong coupling of a macroscopic medium. Currently, there is ongoing research on determining the possible thermalizations of QGP and its equation of state.

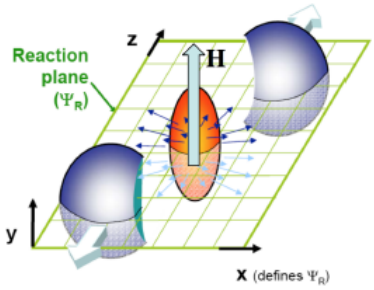

(a) The formation of QGP in off-central collisions. The induced magnetic field is denoted by H.

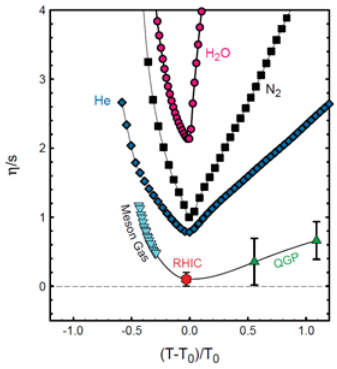

(b) The dimensionless ration $\frac{\eta}{s}$ of shear viscosity with entropy density for H_2O, N_2, He and QGP. T_0 is the critical temperature.

Figure 1.1

In addition to strong coupling, the non-central collisions induce enormous magnetic fields transverse to the reaction plane with magnitudes as large as 10^{19} Gauss. In this case as well as in the interior of dense neutron stars (magnetars) the magnetic field strength probes the scales of strong interactions and plays a considerable role in the dynamics. Ultimately, the effects of the magnetic field are well expected to be observable.

So adding a strong magnetic field can alter significantly the properties

of QCD by adding a new $B-$axis in the $(T-\mu)$ phase diagram (figure 1.2) and produce new phenomena, such as the chiral magnetic effect and inverse magnetic catalysis.

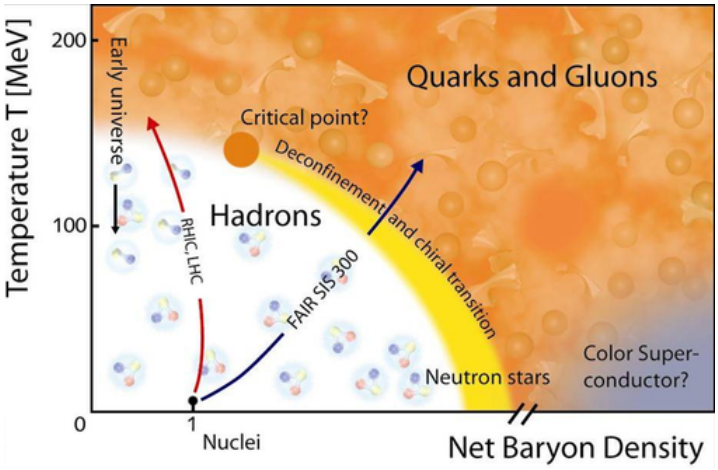

Figure 1.2: The phase diagram of QCD with all its hypothesized phases.

1.2 Lattice QCD

The Lattice Formulation

A full solution of Yang-Mills (YM) theories eludes us till today. Despite asymptotic freedom at high energies, at low energies QCD is strongly coupled and perturbation techniques stand no chance in describing that regime. Even the quark-gluon plasma in the deconfined phase exhibits strong coupling. On top of that, non-perturbative effects are expected to reign in low energies with most intriguing the confinement transition. Not having the analytic tools in our disposal to attack this problem exactly, we resorted to computers. Therefore, based on formulating a gauge theory on a discretized spacetime, *Lattice QCD* is trying to numerically solve the theory[1].

Following Wilson's train of thought, space and time form a lattice of size $N_\sigma^3 \times N_\tau$ with lattice spacing α. The total volume and time are

$$V = (N_\sigma \alpha)^3, \; T = \frac{1}{N_\tau \alpha}.$$

Fermionic fields are now just Grassmanian degrees of freedom on each vertex while gauge fields are defined on the links between them. The action itself S_α

[1] A comprehensive review of this subject can be found in [2].

has a natural cut-off α and is a discretized version of the euclideanized (1.1) up to $\mathcal{O}(\alpha^2)$ deviations that need to vanish in the continuum limit $\alpha \to 0$ and $N_\sigma, N_\tau \to \infty$. Besides some complications in this limit[2], we should be able to extrapolate results to that limit from several lattice sizes.
The central object in Lattice QCD is the partition function

$$Z(V,T,\mu) = \int \mathcal{D}\psi\mathcal{D}\bar{\psi}\mathcal{D}A e^{-S_\alpha[\psi,\bar{\psi},A]}. \tag{1.2}$$

Numerically, Monte-Carlo methods cannot calculate it but derivatives are accessible. However, there are two technical limitations:

- First, computations are feasible only in euclidean time. Analytic continuation to real time is not possible since we are ignorant of the Matsubara poles. Therefore, we can only study static thermodynamics and not non-equilibrium dynamics.

- Second, adding baryon density in the system, namely a chemical potential term $\bar{\psi}\mu\gamma_0\psi$, the fermion operator $\gamma^\mu\partial_\mu - m - \mu\gamma_0$ acquires complex eigenvalues. In turn, its determinant is not strictly positive any more and the numerical methods fail[3]. This is the so-called *sign problem*.

QCD Phase Diagram

Before discussing the thermodynamics of QCD matter as obtained on the lattice, it is essential to go through what is known for the phase transitions taking place.

In theory, there are two kinds of phase transitions: the confinement transition at T_c which signifies that all physical states must be colorless below it and the chiral symmetry breaking at T_χ where the chiral condensate $\left\langle\bar{\psi}\psi\right\rangle$ forms giving rise to $N_f^2 - 1$ pions. These transitions are interconnected but there is a priori no reason for them to coincide. In general, it is expected that $T_c < T_\chi$, as shown in 1.2. The relevant order parameters are the Polyakov Loop $\langle L\rangle$ and the chiral condensate

$$\left\langle\bar{\psi}\psi\right\rangle = \frac{1}{N_\sigma^3 N_\tau}\frac{\partial}{\partial m}\ln Z.$$

[2]The discretised derivative terms $\partial\psi$ leave 16 spurious fermion species rather than 1 in the continuum limit. This *doubling problem* can be bypassed by sacrificing chiral symmetry (Wilson fermions) or by distributing the components of Dirac spinors in several lattice sites (staggered fermions).

[3]As a side note, this obstacle can be evaded for $\frac{\mu}{3} \ll T$.

Useful for determining the order of transition are also their susceptibilities

$$\chi_L = N_\sigma^3 \Big(\big\langle L^2 \big\rangle - \langle L \rangle^2 \Big), \ \chi_m = \frac{\partial}{\partial m} \big\langle \bar{\psi}\psi \big\rangle .$$

Their behaviour is depicted in 1.3. It turns out that both transitions are continuous and almost coincident. In particular, the critical temperature T_c lies in the range $150 - 170$ MeV. Nevertheless, these results strongly depend on the number of flavors and the quark masses. In particular, the deconfining transition changes drastically with the number of flavors. This happens because above T_c the confined degrees of freedom get liberated and enhance the free energy as in figure 1.4.

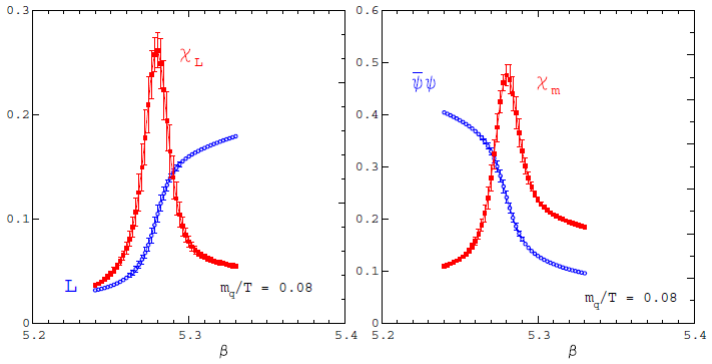

Figure 1.3: The Polyakov loop and the chiral condensate along with their fluctuations as a function of the coupling $\beta = \frac{6}{g^2}$. The peaks of the susceptibilities define the transition points.

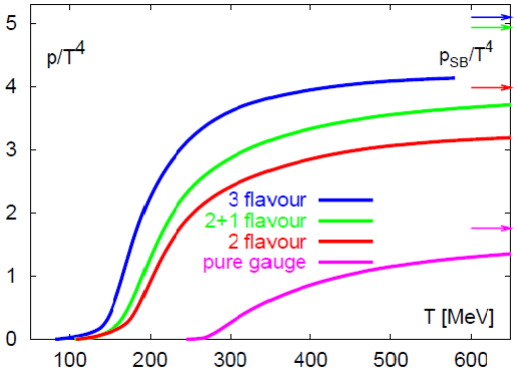

Figure 1.4: The dimensionless pressure as a function of temperature for pure and flavored $SU(3)$. The arrows point to the free-gas limit.

Concerning thermodynamics, the free energy density of the ensemble is

of course

$$\mathcal{F} = -\frac{T}{V} \ln Z.$$

The corresponding pressure is $p = -\mathcal{F}$ and from that all other quantities follow

- Energy density ϵ: $\frac{\epsilon - 3p}{T^4} = T \frac{d}{dT} \left(\frac{p}{T^4} \right)$
- Entropy density s: $\frac{s}{T^3} = \frac{\epsilon + p}{T^4}$
- Sound velocity c_s: $c_s^2 = \frac{dp}{d\epsilon}$

The thermodynamics of pure $SU(3)$ gauge theory are shown in figure 1.5. At large temperature, quarks and gluons are asymptotically free and the plasma approaches the ideal gas. It nearly behaves as a conformal fluid because deviations from $\epsilon = 3p$ by 20% remain even for $T \gg T_c$, probably because of non-perturbative effects.

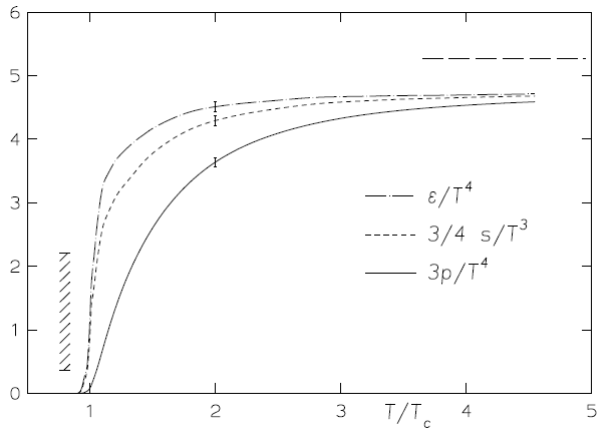

Figure 1.5: The energy, entropy and pressure density for pure $SU(3)$, [3].

Studies with two and three quark flavors have been carried out as well and depicted in figure 1.4. T_c is decreased with increasing N_f. As before, the Stefan-Boltzmann limit is slowly approached.

We conclude by reporting the lattice results on pure $SU(N_c)$ theories for different number of colours N_c, [4]. The figures 1.6 show the thermodynamics for $N_c = 3, 4, 5, 6$ and 8. The agreement is quite surprising suggesting that the structure of the Yang-Mills theory does not change by increasing N_c[4].

[4]As a side note, in the large-N_c limit the confinement-deconfinement crossover becomes a first order phase transition

Worth mentioning it that the thermodynamics is well captured by Improved Holographic QCD, a model to be explained later.

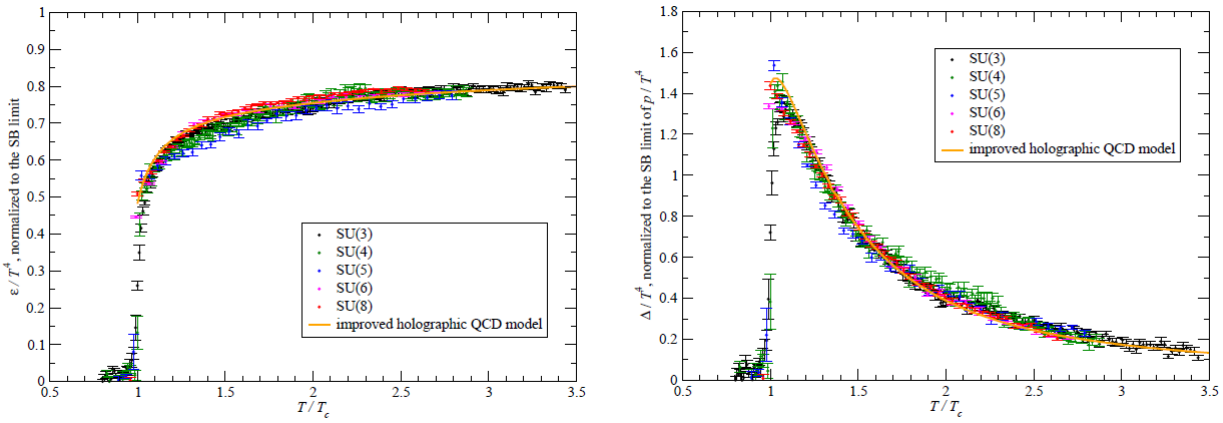

Figure 1.6: The dimensionless energy $\frac{\epsilon}{T^4}$ and conformality measure $\frac{\Delta}{T^4} = \frac{\epsilon - 3p}{T^4}$ versus $\frac{T}{T_c}$ for lattice studies with different N_c and a fitted IHQCD model.

Lattice QCD in Magnetic Field

Recent interest has been focused on shedding light on the properties of QCD in the presence of an external magnetic field. The relevance is obvious for heavy-ion collisions and strongly magnetized neutron stars. The latest studies, [5][5], disprove many of the established ideas about the QCD equation of state in a magnetic field.

First of all, it turns out that the magnetic field does not alter the order of the confinement-deconfinement phase transition at least up to $\sqrt{eB} = 1$ GeV. More interesting, the critical temperature T_c is a decreasing function of B (figure 1.7) in contrast to all low-energy effective theories.

[5]The essential difference from the previous studies is the use of physical quark masses in the simulations.

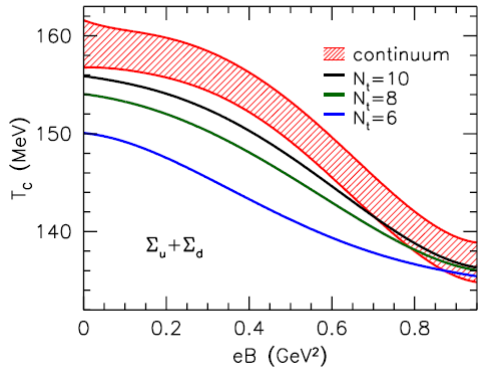

Figure 1.7: $T_c(B)$ in $1+1+1$ flavored QCD. Extrapolation to the continuum is done from $N_\tau = 6, 8$ and 10.

The response to the applied magnetic field was also studied. It was found that the magnetic susceptibility $\chi_B = -\frac{\partial^2 \mathcal{F}}{\partial (eB)^2}|_{eB=0}$ is positive and growing with T around and above T_c. Apart from this paramagnetic phase ($\chi_B > 0$) of QCD, there was found a diamagnetic one ($\chi_B < 0$) at low temperatures where pions dominate and contribute negatively (figure 1.8).

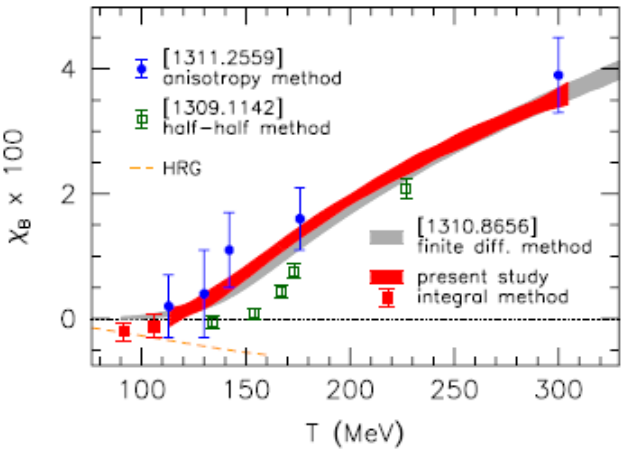

Figure 1.8: The magnetic susceptibility of QCD as a function of T for [5] and other lattice methods.

What is more, as shown in the next figures, the pressure and entropy densities are enhanced by the magnetic field.

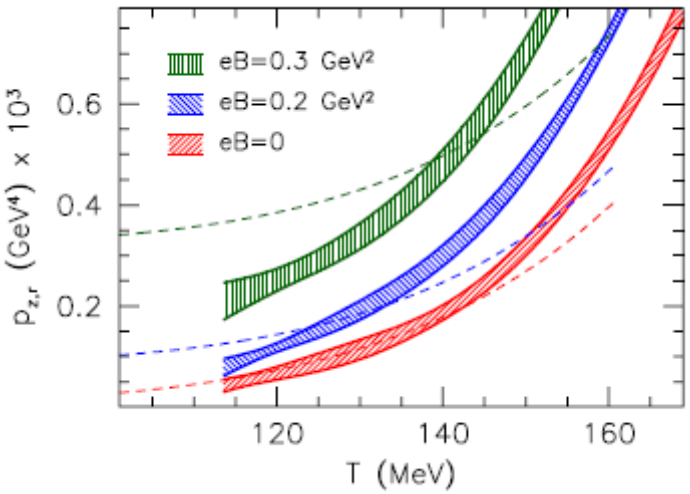

Figure 1.9: Longitudinal pressure (along B) versus T. The dashed lines correspond to the Hardon Resonance Gas model.

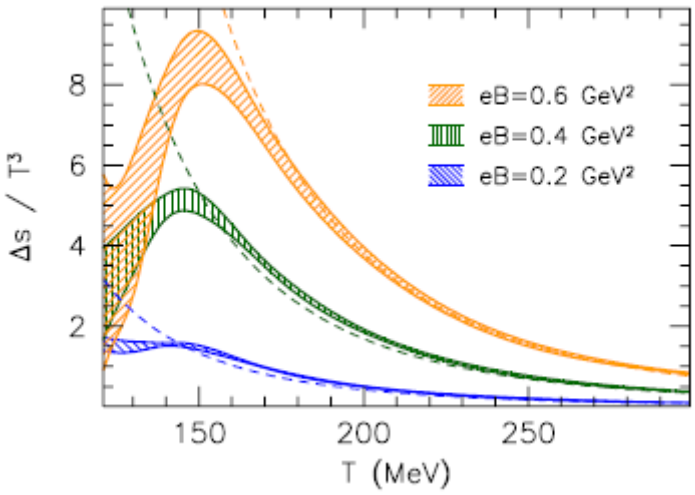

Figure 1.10: Normalized entropy density $\Delta s = s(B) - s(0)$ as a function of T for three different eB values. The dashed lines are the Stefan-Boltzmann limit.

Last but not least, the most intriguing of the results is the behaviour of the chiral condensate for varying B, [6]. While at the $T = 0$ case the magnetic field affects the condensate constructively, an effect coined as *magnetic catalysis*, simulations showed that around the critical temperature the formation of the chiral condensate can be decatalyzed by the magnetic field (figure 1.11). This goes by the name of *inverse magnetic catalysis* and it has

not been predicted by low-energy effective theories probably because of its purely non-perturbative nature.

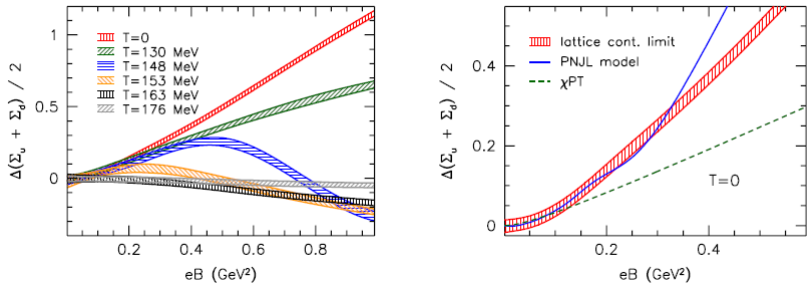

Figure 1.11: Left: The renormalized up and down condensates $\Delta\Sigma_{u,d} \equiv \Sigma_{u,d}(B,T) - \Sigma_{u,d}(0,T)$ as a function of B. Magnetic Decatalysis happens around $T_c = 148$ MeV. Right: Magnetic catalysis at $T = 0$ from lattice simulations, the Nambu-Jona-Lasinio model and chiral perturbation theory.

2 | Quark-Gluon Plasma from Gauge/Gravity Duality

In this chapter we will present the conjecture of AdS/CFT, its formulation, and then what it can tell us about QCD.

2.0.1 The AdS/CFT Correspondence

We start with a type IIB superstring theory in 10 dimensions and we focus on low energies, integrating out all the massive closed string excitations and left only with the massless ones on play.

Adding a stack of N_c D3-branes, the closed strings can break turning into open strings with their endpoints attached to the 3-dimensional subspace of the branes. At low energies, an open string on a Dp brane excites a gauge field A_μ with $\mu = 0, 1, \ldots, p$ and $9 - p$ massless scalar fields ϕ^i corresponding to the deformations of the brane. The configuration of open strings with respect to the N_c coincident Dp-branes produces an $SU(N_c)$ gauge symmetry and in the case of D3-branes the low energy spectrum is an $\mathcal{N} = 4$ super-Yang-Mills (SYM) theory in $3 + 1$ dimensions with gauge group $SU(N_c)$ up to $\ell_s E^2$ higher derivative terms. The coupling constant of the SYM is related to the string coupling as

$$g^2_{\rm YM} = 4\pi g_s. \tag{2.1}$$

Now we consider two limits.

First, the full system consists of interactions between open and closed strings. However, the closed string modes interact with each other and the brane modes through gravity whose coupling constant has dimension E^8. In the low energy limit, the closed and open strings decouple. Further taking the supergravity limit, namely $\ell_s \to 0$ (point-like strings) and $g_s \to 0$ (no quantum string corrections), the gauge theory on the branes becomes pure $\mathcal{N} = 4$ SYM and in the bulk there is a non-interacting type IIB supergravity in flat space. This limit corresponds to $\lambda \equiv g^2_{\rm YM} N_c \ll 1$.

Second, in the supergravity limit of closed strings, the D3-branes source the gravitational background and in the limit of $N_c \to \infty$ they backreact. The supergravity solution of this system describes a spacetime which is Minkowski far from the branes ($r \gg R$) but near them ($r \ll R$) has a "throat"-like geometry

$$ds^2 = \frac{r^2}{R^2}(-dt^2 + dx_1^2 + dx_2^2 + dx_3^2) + \frac{R^2}{r^2}dr^2 + R^2 d\Omega_5^2,$$
$$R^4 = 4\pi g_s N_c \ell_s^4 \text{ (AdS length)},$$

which is an $AdS_5 \times S^5$ geometry. The modes of the asymptotic region are decoupled from the "throat" region. Moreover, in the low energy limit, as perceived from an observer at infinity, we have a non-interacting supergravity at $r \gg R$ but an infinite spectrum of massive fields at $r \ll R$ because their energy is redshifted to zero due to the gravitation potential. Thus, the system reduces to an non-interacting type IIB supergravity in flat space and interacting closed string in $AdS_5 \times S^5$. This is the $\lambda \gg 1$ case.

Identifying that in these two different limits of the same theory the system consists of an interacting and the same non-interacting sector, Maldacena took the leap to put forward that the interacting parts are equivalent, [7]:

Type IIB Superstring theory in $AdS_5 \times S^5 \leftrightarrow$ *$\mathcal{N} = 4$ $SU(N_c)$ SYM theory in* $\mathbb{R}_{3,1} \times S^5$

This is the Anti de Sitter/Conformal Field Theory correspondence. Suppressing the S^5 dependence, the stage of the correspondence is an AdS spacetime where the gravity theory resides in the 5D bulk and the CFT lives in one less dimension on the conformal boundary. The extra, so called holographic, dimension can be identified with the RG flow direction of the CFT. The AdS boundary corresponds to the ultra-violet and the deep bulk to the infra-red.

What makes this correspondence intriguing is that the each side lives in different regimes of the theory. In specific, the SYM is weakly coupled when the 't Hooft coupling constant is small

$$\lambda = g_{\text{YM}}^2 N_c \sim g_s N_c \sim \frac{R^4}{\ell_s^4} \ll 1,$$

whereas the supegravity reduces to classical gravity when the AdS length is larger than the string length

$$\frac{R^4}{\ell_s^4} \gg 1 \to \lambda \gg 1.$$

This is why the correspondence is a *weak-strong duality*. Perturbative results of one side project to strongly coupled results of the other.

Since strongly coupled gauge theories are more interesting to study, the common practice is to consider $\lambda \gg 1$ where the theory in the bulk of AdS is Einstein gravity and standard general relativity techniques can be applied.

2.0.2 The Holographic Dictionary

Formally, AdS/CFT is a correspondence between the partition functions of the conformal theory on the boundary and the supergravity in the bulk.

$$\mathcal{Z}_{CFT} = \mathcal{Z}_{SUGRA}.$$

Especially, in the classical gravity approximation $\mathcal{Z}_{SUGRA}$ will be dominated by the saddles of the action. The relation then becomes

$$\mathcal{Z}_{CFT} = \left\langle \exp\left(\int d^4x J(x)\mathcal{O}_\Delta(x) \right) \right\rangle = e^{-S_{on-shell}[\phi_0]}|_{\phi_0(x,\partial AdS)=J(x)}. \quad (2.2)$$

Some decoding is in order. The communication of the two dual theories is done through the bulk fields $\phi(x,z)$ which act as sources $J(x)$ of local gauge invariant CFT operators $\mathcal{O}_\Delta(x)$ of the gauge theory. Therefore, the on-shell solution of the bulk fields is provided with the physical boundary condition $\lim_{z\to 0}\phi_0(x,z) = J(x)$. This is enough to start using relation (2.2) to calculate correlation functions for the CFT with the standard field theory technology.

Also the symmetry properties of the CFT operators $\mathcal{O}_\Delta$ dictate what the dual bulk fields should be. Unfortunately, even though there is an one-to-one map between operators and fields, there is not a systematic manner of identifying the dual theory.

According to the *field/operator correspondence*, the mass m of the bulk field is tightly related to the conformal weight Δ of the CFT operator and their spins p have to be equal. The general recipe for a AdS_{d+1} bulk is

$$m^2R^2 = (\Delta - p)(\Delta + p - d). \quad (2.3)$$

As an example, the dual of the energy-momentum tensor $T_{\mu\nu}(x)$ is the metric $g_{\mu\nu}(x,z)$.

What is more, since the supergravity action is two-derivative, the equations of motion of the bulk fields are of second order. Assuming for simplicity a scalar field $\phi(x,z)$, its solution near the boundary $z \to 0$ is

$$\phi(\mathrm{x},z) \approx A(\mathrm{x})z^{d-\Delta} + B(\mathrm{x})z^{\Delta}. \quad (2.4)$$

The first term (non-renormalizable mode) blows up and the second (renormalizable mode) vanishes in the UV, $z \to 0$. The integration constants capture the physics of the dual field theory with $A(\mathrm{x})$ being the actual source of $\mathcal{O}_\Delta$ and $B(\mathrm{x})$ its vacuum expectation value $\langle \mathcal{O}_\Delta \rangle$. The former is read from the UV condition and the latter from a regularity condition in the IR.

2.0.3 Generalizations

The concept of AdS/CFT has been generalized in order to extend its original example. The claim is that the bulk geometry can be freely deformed as long as it remains strictly asymptotically AdS. This guarantees the field-operator correspondence and also enriches the RG flow of the boundary theory. We will present two standard kinds of deformations.

Firstly, it would be useful to depart from zero temperature, This would break supersymmetry and conformality and also turn on thermal effects. In the field theory language, this is performed by euclideanising the time direction and making it periodic,

$$t \to i\tau \text{ with } \tau \sim \tau + \beta$$

where $\beta = \frac{1}{T}$ is the inverse temperature. The zeroth example of this is applying that to pure AdS. The new solution is called *thermal gas solution* and in Poincaré coordinates is

$$ds^2 = \frac{d\tau^2 + dz^2 + d\vec{x}^2}{z^2}.$$

The temperature T is arbitrary and the thermodynamics are actually empty. It is a zero entropy state.
The next example is the *AdS black hole solution*,

$$ds^2 = \frac{f(z)d\tau^2 + \frac{dz^2}{f(z)} + d\vec{x}^2}{z^2}.$$

The spacetime now has an event horizon at z_h where $f(z_h) = 0$ and differs substantially from the thermal gas because of the regularity conditions on the horizon and also other IR effects we will see in the next sections.
Expanding near the horizon, $f(z) \approx f'(z_h)(z - z_h)$, the geometry is

$$ds^2 \sim f'(z_h)(z-z_h)d\tau^2 + \frac{dz^2}{f'(z_h)(z-z_h)} \overset{dz=\sqrt{f'(z_h)(z-z_h)}d\rho}{=} \rho^2 \frac{f'^2(z_h)}{4} d\tau^2 + d\rho^2.$$

In order to avoid the conical singularity at $\rho = 0$, imaginary time acquires periodicity $\beta = \frac{4\pi}{|f'(z_h)|}$. So the black hole is associated with a Hawking

temperature. At last, black hole thermodynamics come to use as they are inherited by the boundary theory.
More specifically, entropy follows the Bekenstein formula

$$S = \frac{\mathcal{A}_h}{4G_{d+1}} = \frac{1}{4G_{d+1}} \int_{z_h} d^{d-1}x\sqrt{h}$$

and is proportional to N_c^2.

Secondly, according to the holographic dictionary, local symmetries of the bulk imply global symmetries on the boundary. Thus, adding a U(1) gauge field A in the bulk implies a conserved charge on the boundary, e.g. the charge of the quark-gluon plasma.
Because the charge density Q is the zeroth component of the conserved current, only that component is turned on:

$$A = A_t(r)dt,$$

which is an electric field $A_t'(r)$ along the holographic direction. The total charge Q_{tot} is measured at infinity

$$Q_{\text{tot}} = \frac{1}{4\pi G_{d+1}} \lim_{r\to+\infty} \int d^{d-1}x\sqrt{h}NF^{0\nu}n_\nu,$$

where $h_{\mu\nu}$ is the boundary induced metric, N is the lapse function and n_ν the normal vector to the boundary.
The associated chemical potential to Q is the work needed to bring a test particle from the horizon to the boundary,

$$\mu = \int_{r_h}^{+\infty} A_t'(r)dr = \lim_{r\to+\infty} A_t(r) - A_t(r_h).$$

Finally, getting back to the 1st law of thermodynamics for a black hole of mass M and charge Q in the grand canonical ensemble, it reads

$$dM = TdS + \mu dQ.$$

In order to consider a grand canonical ensemble we need to keep T and $\mu = A_0(r \to \infty)$ fixed. This is implemented by adding a boundary *Gibbons-Hawking term* into the action

$$S = \frac{1}{16\pi} \int_{\mathcal{M}} d^{d+1}x\left(R - \frac{1}{4}F^2\right) + \frac{1}{8\pi} \int_{\partial\mathcal{M}} d^dx\sqrt{h}K, \tag{2.5}$$

where $h_{\mu\nu}$ is the induced metric on $\partial\mathcal{M}$ and $K = h^{\mu\nu}\nabla_\mu n_\nu$ its extrinsic curvature. This boundary term does not affect the equations of motion but

cancels the contribution of the first derivatives of the metric on the boundary making the variational problem well-defined. Varying (2.5) with respect to $g_{\mu\nu}$ and A_μ yields

$$\delta S = \Big(\text{E.O.M.}\Big)[\delta g_{\mu\nu}, \delta A_\mu] + \Big(\text{gravitational boundary term}\Big)\delta g^{\mu\nu} - \frac{1}{16\pi}\int_{\partial\mathcal{M}} d^d x\sqrt{h}F^{\mu\nu}n_\mu \delta A_\nu$$

For the equations of motion to remains intact we take $\delta A_\mu(r \to \infty) = 0$, hence fixing the chemical potential. Ultimately, the grand canonical potential is

$$\mathcal{F} = M - TS - \mu Q. \tag{2.6}$$

Adding other boundary terms in the action, one can switch to other ensembles.

2.0.4 AdS/CFT Correspondence and QCD

The gauge/gravity duality offers a new framework to tackle strongly coupled problems and has the asset of allowing real time and non-zero chemical potential in contrast to lattice QCD. Even though we lack a full description of AdS/CFT we can still learn qualitative and universal properties that strongly coupled large-N_c theories might share and become wiser in that respect. Nevertheless, of foremost also importance is the relevance of this correspondence with real world physics. The quark-gluon plasma seems to be strongly coupled but is a holographic description of it justified? In other words, can we smoothly deform the correspondence such that the dual large-N_c SYM theories approximate QCD as we know it, an SU(3) YM Theory, and how much can we approach it?
Before proceeding with suggested holographic models, it is worth stressing the fundamental gaps that have to be surpassed. The following points summarize the differences:

- SYM is glue-dominated with $N_c \to \infty$, while for QCD $N_c = 3$. From the discussion at page 10, 3 is likely not to be such a "small" number after all. However, including $\mathcal{O}(\frac{1}{N_c^2})$ corrections from considering higher derivative terms in the gravity side gives a better scope.

- The entire particle spectrum, including fermions, in SYM lives in the adjoint representation of the gauge group. In QCD, on the other hand, quarks live in the fundamental representation. As a result, QCD has a chiral condensate while SYM cannot incorporate one.

- SYM is maximally supersymmetric whereas QCD is not.
- SYM is conformal and thus has a tunable coupling while QCD has a running coupling constant.
- QCD is confining at low energies while SYM is not.

Notwithstanding these very big differences between the theories, ways have been devised such that we give up the superfluous symmetry, namely conformality and supersymmetry, such that the bulk theory can describe a better toy model of QCD. What is more compelling a question is how to describe confinement from the gravity side and account for physical fermions in the boundary theory.

2.0.5 Confinement

The most physically essential task is to decode the holographic realization of the confinement phase transition. In a gauge theory, a class of non-local gauge invariant quantity that encloses non-perturbative effects of the theory is the *Wilson line*,

$$W(\mathcal{C}) = \text{Tr } \mathcal{P} e^{i \int_{\mathcal{C}} A},$$

where A is the gauge connection, the trace over the chosen representation of $SU(N)$ and $\mathcal{P}$ the path-ordering along the $4D$ path $\mathcal{C}$.
It can be shown that in the case of static, equivalently infinitely massive quarks, and large time distance $\mathcal{T}$ the amplitude of a quark propagating along $\mathcal{C}$ is actually the expectation value of the Wilson line. This means that

$$\langle W(\mathcal{C}) \rangle \sim e^{-iM_q \mathcal{T}}.$$

As a next step, closing the contour, $\mathcal{C}$ is then the boundary of the worldsheet swept by a string connecting a quark and an antiquark. Now the expectation value is related to the total energy of a quark-antiquark pair. In the static case,

$$\langle W(\mathcal{C}) \rangle \sim e^{-iE_{tot}\mathcal{T}} = e^{-i(M_q + V_{q\bar{q}})\mathcal{T}}.$$

The mass term can be regularized and does not influence the following discussion.

A confined quark-antiquark pair is characterized by an attractive potential linear to their distance, that is $V_{q\bar{q}} \propto L$, or, put in different words, by an area law for the Wilson loop. This is a criterion for confinement.

There is a dual description of the previous picture in a string theory in $4 + 1$ dimensions. As known, fundamental matter is introduced by adding

D-branes in the bulk with open strings attached to it. The open-string endpoints on the D-brane represent quarks charged under the gauge group while its position in the radial direction is proportional to the quark mass. Now the worldline of the quark $\mathcal{C}$ constitutes the boundary of the open-string worldsheet Σ (figure 2.1). AdS/CFT suggests that the expectation value of the Wilson loop is equal to the on-shell partition function of the corresponding worldsheet action in the large-N_c, large-λ limit,

$$\langle W(\mathcal{C})\rangle = e^{iS_{on-shell}(\partial\Sigma=\mathcal{C})}.$$

The problem now is reduced to area minimization. This equation tells us a lot about how to qualitatively choose the background geometry that signals confinement. Embedding the string in spaces with different IR asymptotics we read off different interaction potentials for the quarks. The standard example of pure AdS yields the expected conformal result $V_{q\bar{q}} \propto \frac{1}{L}$.

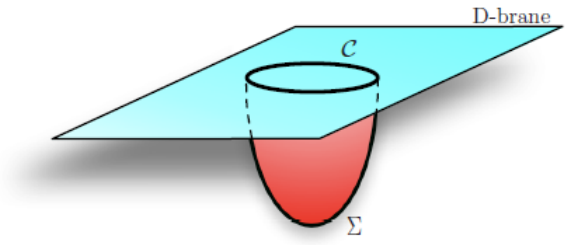

Figure 2.1: The string worldsheet associated to the Wilson loop $\mathcal{C}$. Taken from [8].

If there is an IR cut-off z_{IR} where spacetime terminates abruptly, separating the quarks enough from each other brings the string connecting them closer to this "Hard Wall". It turns out that the minimal surface is achieved for the string lying along the IR cut-off with the area of the worldsheet being directly proportional to $L\mathcal{T}$, yielding the desired area law (figure 2.2).
In the presence of a black hole horizon z_h things get more interesting. When the horizon reaches a critical z_c, the string connecting the quarks would rather break in two straight strings extending from each quark to the horizon (figure 2.2). This signals deconfinement, the quarks are free. Without sweat, we see that black holes should always be associated with a transition temperature T_c towards deconfinement.

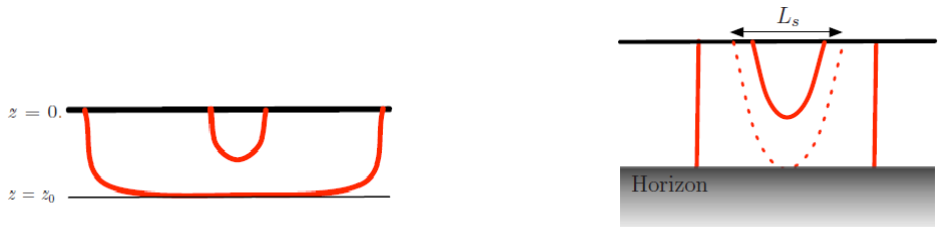

Figure 2.2: The string in a space with an IR cut-off (left) and a black hole (right). Taken from [8].

In a field theory without fundamental matter, confinement is identified with the spontaneous breaking of the center Z_{N_c} of the Gauge group. The relevant order parameter of this phase transition is the *Polyakov Loop*, a Wilson line wrapped around the compactified time direction at a specific spatial point, which transforms nontrivially under Z_{N_c}. In the confined phase $\langle W(\mathcal{C})\rangle = 0$ while in the deconfined phase $\langle W(\mathcal{C})\rangle$ is non-zero. If quarks are included in the system then the Polyakov Loop is not a proper order parameter any more but in the large-N_c limit is replaced by the N_c dependence of the free energy $\mathcal{F}$. In color-confined phase, $\mathcal{F}$ is dominated by the gluons, so $\mathcal{F} \sim \mathcal{O}(N_c^2)$ whereas in the deconfined phase $\mathcal{F} \sim \mathcal{O}(1)$.

Witten reasoned that holographically this phase transition is realised as a Hawking-Page transition between a Thermal Gas geometry and an AdS-Schwarzschild Black Hole, [10]. This can be seen in two different ways. First, the free energy of a black hole is proportional to its entropy which holographically is of $\mathcal{O}(N_c^2)$. From a Polyakov loop point of view, in the AdS-vacuum the string worldsheet can probe indefinitely deep in the bulk, vanishing thus the Polyakov loop exponentially. In a black-hole phase the worldsheet terminates at the horizon, giving a non-zero Polyakov loop expectation value.

2.0.6 Fundamental Matter in AdS/CFT

The theory on the AdS boundary is pure Yang-Mills as N_c is taken to infinity while keeping $\lambda = g_{YM}^2 N_c$ fixed. Obviously, this limit is far from reality because flavor quarks are missing at all. In the QCD-language this means we are working in the quenched approximation where the quark loops are suppressed. It is vital to endow our dual model with a flavor sector in order to resemble more QCD.

According to the large-N_c limit, quarks are represented by one-line propagators in the two-line representation introducing boundaries in the 't Hooft expansion. This amounts to adding open strings in the bulk. So, besides

the N_c color $D3-$branes, we now need to add a stack of N_f overlapping $Dp-\bar{D}p$ "flavor" brane-antibrane pairs, [9]. Depending on what branes the open strings are attached to we have three types: $3-3$, $3-p$ (or $p-3$) and $p-p$. At low energies, $3-3$ strings give the $\mathcal{N}=4$ SYM multiplet in the adjoint of $SU(N_c)$. The $3-p$ strings give degrees of freedom transforming in the bifundamental of $SU(N_c)\times SU(N_f)$ while the $p-p$ in the bifundamental of $SU(N_f)\times SU(N_f)$. The coupling constant for the $p-p$ strings scales as E^{p-3}. So for $p>3$, the $p-p$ strings become non-interacting at low energies and the local symmetry $SU(N_f)$ becomes global symmetry.

In the limit $\lambda \ll 1$ and low energies we have two decoupled sectors. First, free closed strings propagating in 10D flat space and $p-p$ strings propagating on the worldvolume of N_f Dp-branes. Second, we have the light degrees of freedom from the $3-3$ and $3-p$ strings interacting with each other. In the limit of $\lambda \gg 1$, we have a different picture. At low energies, we have closed and $p-p$ strings propagating in two decoupled regions: the asymptotically flat region and the $AdS_5\times S^5$ near the branes. The former region is free whereas the latter is interacting. Once again, by identifying the free sectors of the two limits, we proceed to conjecture that the interacting sectors are descriptions of the same thing. Therefore, we conjecture that the $\mathcal{N}=4$ SYM coupled to N_f flavors of fundamental degrees of freedom is dual to type IIB closed strings in $AdS_5\times S^5$, coupled to open strings propagating on the worldvolume of N_f $Dp-$branes.
The dynamics on the flavor branes are dictated by the open string action $S_f = S_{\rm DBI}+S_{\rm WZ}$. In the string frame, the non-abelian Dirac-Born-Infeld (DBI) action[1] reads

$$S_{\rm DBI} = -\frac{1}{2}M_p^3 N_c \int d^{p+1}x \mathbf{STr}\left[e^{-\phi}V(TT^\dagger, Y_L^I - Y_R^I, x)(\sqrt{-\det \mathbf{A_L}}+\sqrt{-\det \mathbf{A_R}})\right], \tag{2.7}$$

where

$$A_{(i)MN} = g_{MN}+B_{MN}+F^{(i)}_{MN}+\partial_M Y^I_{(i)}\partial_N Y^I_{(i)}+\frac{2}{\pi}(D_{\{M}T^\dagger)(D_{N\}}T),$$

with

$$F^{L/R} = dA^{L/R} - iA^{L/R}\wedge A^{L/R},\ D_M T = (\partial_M + iA^L_M - iA^R_M)T.$$

Here ϕ is the closed string dilaton, $A^{L/R}$ are the non-abelian worldsheet gauge fields and T is a complex scalar transforming in the bifundamental

[1]Throughout the discussion, we will be using this version of the DBI action proposed by Sen and others.

representation of $U(N_f)_L \times U(N_f)_R$ which we shall call Tachyon for reasons that will become obvious soon. The background $B-$field and the transverse scalars $Y^I_{L/R}$ of the brane we will set to zero for the rest because they don't have a known analogue in QCD, thus they do not serve for our purposes. The remaining $T, A^{L/R}$ fields are dual to gauge invariant operators formed by quark bilinears and also the system has a built-in flavor symmetry $U(N_f)_L \times U(N_f)_R$.

The Wess-Zumino topological action $S_{\rm WZ}$ descibing the coupling of the (anti-)branes to the background RR potentials is

$$S_{\rm WZ} = T_p \int_{\Sigma_{p+1}} C \wedge str\, \exp[i2\pi\alpha' \mathcal{F}]. \tag{2.8}$$

Σ_{p+1} is the world-volume of the Dp-$\bar{D}p$ branes, C is a formal sum of the RR potentials $C = \sum_n (-i)^{\frac{5-n}{2}} C_n$ and $\mathcal{F}$ is the curvature of a superconnection $\mathcal{A}$ defined as

$$\mathcal{F} = \mathrm{d}\mathcal{A} - i\mathcal{A}\wedge\mathcal{A},\ \mathrm{d}\mathcal{F} - i\mathcal{A}\wedge\mathcal{F} + i\mathcal{F}\wedge\mathcal{A} = 0.$$

In terms of the tachyon T and the gauges fields $A^{L/R}$

$$i\mathcal{A} = \begin{pmatrix} iA_L & T^\dagger \\ T & iA_R \end{pmatrix}, \quad i\mathcal{F} = \begin{pmatrix} iF_L - T^\dagger T & DT^\dagger \\ DT & iF_R - TT^\dagger \end{pmatrix}.$$

The Wess-Zumino action captures the discrete symmetries (P, C) on the branes. From the dual theory point of view, the Wess-Zumino term reproduces the $U(1)_A$ anomaly and enforces chiral symmetry breaking in confining backgrounds.

A common practice in AdS/CFT is to consider $N_f \ll N_c$, treating the flavor branes as probes not backreacting to the $D3-$brane background. Going beyond the quenched approximation would mean to add more flavor branes, comparable as a number with N_c. This is consistently formulated in the *Veneziano Limit*, where the number of flavors is taken to infinity while keeping $\frac{N_f}{N_c} \sim \mathcal{O}(1)$. In this way the system is more realistic but also more complicated.

In this new "large-N_f limit", comparison with QCD is meaningful only in terms of the ratio $\chi_f = \frac{N_f}{N_c}$, which for QCD itself is $\chi_f = \frac{6}{3} = 2$. The physics is now also dependent on χ_f which comes as a multiplier in front of S_f and works as an on-off switch for the flavor branes[2]. This dependence is not

[2]To see that more clearly, in the vacuum state where the gauge fields can be taken zero and the tachyon diagonal in flavor space, $T(r) = \tau(r)\mathbb{I}_{N_f\times N_f}$, then the L and R brane actions become identical and tracing over the gauge indices gives an overall N_f factor.

trivial and it can drive the theory to interesting new regimes. In particular, the existence of a "conformal window" $\chi_c < \chi_f < \frac{11}{2}$ has been shown, where there is a nontrivial IR fixed point and the theory becomes weakly coupled as $\chi_f \to \frac{11}{2}$. Below χ_c chiral symmetry breaking takes place while near χ_c the coupling constant "walks" towards the IR fixed point.

3 | AdS/QCD

The Top-Down and Bottom-Up Models

Holographic models are divided into two categories, each following different philosophy in describing the dual theory. These are the top-down and bottom-up models.

On the one hand, the top-down models constitute extensions of Maldacena's proposal in a quantum gravity framework. Namely, the bulk theory is a consistent solution of a low-energy effective supergravity theory descending from a critical string theory. One then, following very exact considerations, models a dual theory with the desired properties.

The first attempt to a QCD-like dual in that manner was made by Witten, [10]. Assuming a Type IIA string theory, N_c $D4-$branes were considered instead of $D3$ ones. The gauge theory on the branes is of course a five dimensional supersymmetric $SU(N_c)$ gauge theory with fermions and scalars in the adjoint representation. Compactifying one spacelike direction on a circle of radius M_{KK}^{-1} with anti-periodic boundary conditions for the fermions supersymmetry is broken and the fermions acquire mass at tree-level and the scalars at one-loop. Only the gauge fields zero modes around the circle remain massless due to gauge invariance and finally prevail at energies lower than the energy scale M_{KK}. Therefore, for $E \ll M_{KK}$ the theory is a pure four dimensional $SU(N_c)$ gauge theory. In addition to this, the background sourced by the $D4-$branes has the peculiarity that the holographic radius terminates smoothly at some U_Λ giving a "cigar" shape to the geometry. Thanks to this IR-wall the theory exhibits confinement. All this elaborate construction manages to reproduce features of QCD IR dynamics but still at higher energies physically fails because of the infinite towers of Kaluza-Klein modes.

Restricting to the low energy sector, if one wishes to find out the mesonic spectrum of this model, adding flavor branes is indispensable. At the popular *Sakai-Sugimoto model* [11], stacks of N_f $D8$ and $\bar{D}8$ probe branes are embedded in the $D4$ background at two different points of the circle. As long

as the two stacks are disconnected we have a symmetry $U(N_f)_L \times U(N_f)_R$ and chiral symmetry is manifested on the flavor brane world-volume. Chiral symmetry breaking can be easily visualized. In the confined phase the geometry forces the branes and antibranes to recombine, thus breaking chiral symmetry to the subset $U(N_f)_{L+R}$, whereas embedded in a non-zero temperature black hole geometry the stacks fall into the horizon remaining distinct, preserving the symmetry (figure 3.1). This model gives N_f^2 Goldstone bosons and several quantities, such as meson masses, decay constants and couplings, are in reasonable agreement with observations. Nevertheless, it lacks parameters directly connected to the quark bare masses and the chiral condensate as well as massive pions.

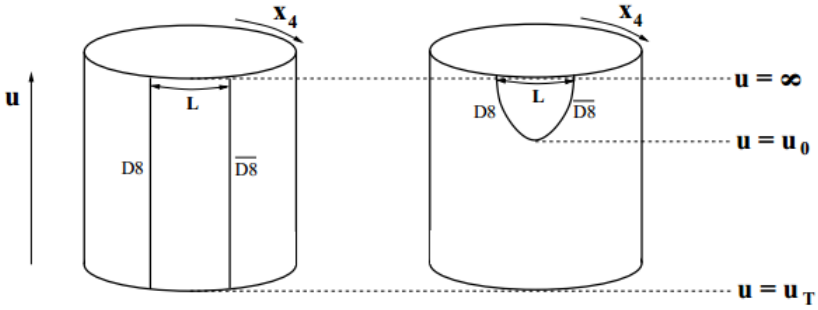

Figure 3.1: The Sakai-Sugimoto model. Left: the chirally symmetric phase with the D8−branes ending at the black hole horizon u_T. The gauge symmetry is $U(N_f)_L \times U(N_f)_R$. Right: the chirally broken phase with the branes recombining with the anti-branes at u_0 with u_T the tip of the spacetime. The gauge symmetry is $U(N_f)_{L+R}$. Taken from [13].

On the other hand, there is an alternative way of creating holographic models. The bottom-up approach is founded on moulding the gravitational theory at will, not necessarily emerging from a string theory, so that the dual theory has specific properties. This "elastic" yet self-consistent way of thinking, free of string theoretical restrictions, is of course "phenomenological" but manages to capture many qualitative features of QCD.

The story started in [14] where a five-dimensional AdS space with an abrupt IR cut-off was studied. This cut-off breaks conformality and also guarantees confinement and a mass gap. The field content includes a chiral condensate and mesons read directly from the holographic dictionary. Chiral symmetry breaking was imposed by hand and yielded a good matching of the meson spectrum by satisfying the Gell-Mann-Oakes-Renner relation. However, the glueball spectrum does not coincide with the lattice data. Apart

from its drawbacks, this conceptually simple model sparkled interest towards that direction. Later in [15], the crude hard IR wall was softened by a dilaton which effectively suppressed the deep IR and set a characteristic scale for that. This model was successful in producing linear Regge trajectories for the mesons but since it was not dynamical itself black hole thermodynamics would not hold rending many calculated quantities unreliable.

The previous models share the shortcoming of not describing fully cousins of QCD. For instance, they both do not account for a running coupling constant and as a result the asymptotic freedom in the UV is absent. So the question arises in what context one has to work in order to take into account all the known properties of QCD. This brings us to *Improved Holographic QCD* (IHQCD), the AdS/QCD model considered in this thesis.

Improved Holographic QCD

Improved Holographic QCD was first proposed in [16] and the basic idea is to build the most economic set-up to simulate a pure large-N_c Yang Mills theory. Inspired by non-critical string theories, it is formulated in five dimensions, four Minkowski plus the holographic one representing the RG scale. Its field content is also minimal: a metric function $g_{\mu\nu}$ dual to the stress-energy tensor of the "glue" $T_{\mu\nu} = F_{\mu}^{\rho}F_{\rho\nu} - \frac{\delta_{\mu\nu}}{4}F^2$ and a scalar field, the dilaton ϕ, dual to the gluon condensate TrF^2.

We will now present the gravitational action in the Einstein frame and immediately try to understand it,

$$S_g = -\frac{1}{16\pi G_5}\int_{\mathcal{M}} d^5x\sqrt{-g}\left(R - \frac{4}{3}(\partial\phi)^2 + V(\phi)\right) + \frac{1}{8\pi G_5}\int_{\partial\mathcal{M}} d^4x\sqrt{-h}K. \tag{3.1}$$

This is a two-derivative Einstein-Dilaton action with a boundary Gibbons-Hawking term to make the variational problem well-defined.
The role of the dilaton is crucial for the physics of the dual theory. We will identify it with the 't Hooft coupling[1] as $\lambda = N_c g_{YM}^2 \equiv e^{\phi}$ and its potential $V(\phi)$ will take care of its running. Therein lies the novelty of IHQCD. By requiring confinement in the IR, idea borrowed from the soft wall model, and asymptotic freedom in the UV, one can construct classes of potentials reproducing those two vital features of QCD. Here we will quickly review how this is done. Detailed derivations of the results can be found in [16].

Consider a euclideanised vacuum solution in conformal coordinates,

$$ds_0^2 = e^{2A_0(r)}\left(dt^2 + dr^2 + d\vec{x}^2\right),\ \lambda_0(r) \tag{3.2}$$

[1]By convention, we will call $\lambda(r) = e^{\phi(r)}$ the dilaton and all the dynamics will be expressed in terms of it even though ϕ is dual to $\mathrm{Tr}F^2$.

where $A_0(r)$ is identified with the energy scale and the dynamical $\lambda(r)$ with the 't Hooft coupling constant. Einstein equations imply that $A_0''(r) < 0$ which along with the requirement of asymptotic AdS-ness, that is $A_0 \sim \ln r$ as $r \to 0$, justify $A_0(r)$ as the holographic energy scale. One can then define the *holographic beta function*

$$\beta(\lambda) = \frac{d\lambda}{d\log E} \tag{3.3}$$

which is exclusively dependent on the form of $V(\lambda)$.
Knowledge of the Yang-Mills beta function $\beta^{\rm YM}(\lambda)$ in the perturbative UV regime allows an one-to-one matching with $\beta(\lambda)$. To be more specific, the one-loop beta function is

$$\beta^{\rm YM}_{1-\rm loop}(g) = \frac{dg}{d\log E} = -\frac{11}{3}\frac{N_c}{(4\pi)^2}g^3$$

and as a function of the 't Hooft coupling,

$$\beta^{\rm YM}_{1-\rm loop}(\lambda) = \frac{d\lambda}{d\log E} = -\frac{22}{3}\frac{\lambda^2}{(4\pi)^2}.$$

The last equation has the well-known solution of a logarithmically vanishing λ,

$$\lambda(E) = \frac{3(4\pi)^2}{22\log\left(E/_{\Lambda_{\rm QCD}}\right)}.$$

This gives the hint that e^{ϕ} has to vanish logarithmically as $A_0 \to -\infty$. More generally, for a dilaton potential with a regular expansion around $\lambda = 0$,

$$V(\lambda) = \frac{12}{\ell^2}(1 + u_0\lambda + u_1\lambda^2 + \dots),$$

(3.3) has an expansion $\beta(\lambda) = -b_0\lambda^2 - b_1\lambda^3 + \dots$ with $b_0 = \frac{9}{8}u_0$ and $b_1 = \frac{9}{4}u_1 - \frac{207}{256}u_0^2$. Matching term by term with $\beta^{\rm YM}(\lambda) = -\frac{22}{3(4\pi)^2}\lambda^2 - \frac{68}{3(4\pi)^4}\lambda^3 + \dots$ up to 2 loops[2] gives us the values of the coefficients u_0, u_1 in an universal way. It is also notable that this very procedure introduces logarithmic contributions to the UV asymptotics of the metric and the dilaton. Finally, the spacetimes in IHQCD turn out to be *logarithmically asymptotically AdS*, behaving at the boundary ($r \to \infty$) as

$$ds_0^2 = \frac{\ell^2}{r^2}\left(1 + \frac{8}{9}\frac{1}{\log r\Lambda} + \dots\right)\left(dt^2 + dr^2 + d\vec{x}^2\right),\ \lambda_0 = -\frac{1}{\log r\Lambda} + \dots,$$

[2]The next coefficients b_i of QCD are scheme-dependent.

where Λ is the integration constant of the dilaton and physically corresponds to the strong coupling scale Λ_{QCD} of the dual theory. Formally it is defined as

$$\Lambda_{\rm QCD} = \ell^{-1} \lim_{\lambda\to 0}\left[e^{A(\lambda)}\frac{\exp\left(-\frac{1}{b_0\lambda}\right)}{\lambda^{b_1/b_0^2}}\right]. \tag{3.4}$$

Having assured the desired UV asymptotics, we turn to the non-perturbative IR phenomena, such as confinement. This task is based on the Wilson-loop test and is discussed in the Appendix A. The result is that in the deep IR, large λ limit, confinement and magnetic charge screening require that

$$V(\lambda) \sim \lambda^{2Q}(\log\lambda)^P \text{ with } Q = \frac{2}{3} \text{ and } P \geq 0.$$

As a by product, the excitation spectrum is $m^2_{\rm mesons} \sim n^{2P}$.
Stitching those asymptotic behaviours smoothly picks a number of admissible potentials. We just need to cook up one that interpolates between these asymptotics and produces linear Regge trajectories $m^2_{\rm mesons} \sim n$.

Passing on to the thermodynamics, there are two thermal solutions of the system:

- The thermal gas solution (TG), governed by the vacuum solution (3.2) just discussed, which corresponds to the confined phase of the gauge theory.

- The black hole solution (BH), corresponding to the deconfined phase,

$$ds^2 = e^{2A(r)}\left(f(r)dt^2 + \frac{dr^2}{f(r)} + d\vec{x}^2\right),\ \phi(r)$$

  where there is a horizon r_h such that $f(r_h) = 0$.

The black hole case does not differ much from the thermal gas since it still preserves asymptotic freedom in the UV. However, its horizon provide the thermodynamics of the dual theory while in the thermal gas case even temperature is arbitrary. The two phase compete with each other for the minimum energy state. The phase transition is signalled by the change of sign in their free energy difference, which for AdS/CFT means

$$\beta\Delta\mathcal{F} = \beta\Big(\mathcal{F}_{BH} - \mathcal{F}_{TG}\Big) = S_{BH} - S_{TG}. \tag{3.5}$$

There are subtleties in this simple formula. First of all, we know that in asymptotically AdS spaces the on-shell actions diverge. The common practice is to regularize the action by adding counterterms on some UV cut-off.

However, since those divergences stem from the near boundary geometry, they are the same for BH and TG and will cancel out in (3.5). Still it has to be assured that this subtraction has a physical meaning, that is both geometries describe the same class of boundary theories. The parameter characterizing each theory is the $\Lambda_{\rm QCD}$ dilaton integration constant and has to be the same in such comparisons. In addition to that, the proper time and space lengths should coincide. In total, defining two UV cut-offs ϵ_0 and ϵ we require:

- Proper time length: $\beta_0 e^{A_0(r)}|_{\epsilon_0} = \beta e^{A(r)}\sqrt{f(r)}|_{\epsilon}$
- Proper 3-D space volume: $V_3^0 e^{3A_0(r)}|_{\epsilon_0} = V_3 e^{3A(r)}|_{\epsilon}$
- Λ_{QCD}: $\lambda_0(\epsilon_0) = \lambda(\epsilon)$

The phase structure of the system is interesting. Thanks to the symmetries of the equations every black hole solution is solely parametrized by the dilaton value λ_h at the horizon. It turns out that there is a temperature $T_{\rm min}$ below which only the thermal gas exists. Above two black hole branches appear, the “big" black holes and the “small" black holes. The former is thermodynamically stable with specific heat $c_u = T\frac{dS}{dT} > 0$ and the latter not. As one might physically expect for QCD matter, thermal gas (confinement) prevails at low temperature while at a critical $T_c > T_{\rm min}$ big black holes take over deconfining the theory through a Hawking-Page phase transition, [17]. This transition is similar to the deconfinement transition of large$-N_c$ YM theories: it is of first order and at high temperatures the system asymptotes to the Stefan-Boltzmann limit $\mathcal{F}_{SB} = -\frac{\pi^2}{45}N_c^2T^4$, like a free gluon plasma.

Ultimately, a comparison with the lattice data is vital and the fitting turns out to be strikingly good, [4, 19]. Normalization to the Stefan-Boltzmann limit sets the Planck Mass $(M_p\ell)^3 = \frac{1}{45\pi^2}$ while adjusting the dilaton potential $V(\lambda) = \frac{12}{\ell}\Big(1+V_0\lambda+V_1\lambda^{4/3}\sqrt{\log\Big[1+V_2\lambda^{4/3}+V_3\lambda^2\Big]}\Big)$ succeeds in reproducing quantitatively[3] the thermodynamics in the confined and deconfined phase as well (figure 1.6).

To conclude, Improved Holographic QCD offers an unexpectedly reliable phenomenological model of large-N_c YM theories at thermal equilibrium and probably a valid way to study the quark-gluon plasma. Many extensions to it have been considered, such as calculating transport coefficients and adding flavor. The latter is the core of this thesis.

[3] In fact, all quantities appear in units of the string length l_s. By setting l_s to reproduce exactly the lattice value of $T_c = 155$ MeV all other quantities become dimensionfull.

4 | The Holographic Models

We used two bulk theories, dual to different field theories, and studied how their thermodynamics change in the presence of an external magnetic field. For the first theory we know the dual and the second is more relevant to QCD.

4.1 The Kraus-D'Hoker Model

One of the first holographic duals of a $3+1$ gauge theory with constant magnetic field was proposed in [24]. There the bosonic part of $D=5$ minimal gauge supergravity was considered,

$$S=-\frac{1}{16\pi G_5}\int \mathrm{d}^5x\sqrt{-g}\left(R+F^{\mu\nu}F_{\mu\nu}-\frac{12}{L^2}\right)+S_{GH}+S_{CS}, \tag{4.1}$$

where $F=dA$, $L=1$ is the AdS length, S_{GH} is the boundary Gibbons-Hawking term and the Chern-Simons term

$$S_{CS}=\frac{k}{16\pi G_5}\int A\wedge F\wedge F,\ k=\frac{8}{3\sqrt{3}}.$$

What is fortunate is that this gravity theory has a specific dual, a consistent truncation of $D=5$ $\mathcal{N}=4$ SYM. There is no dilaton, and then no sense of confinement.

We consider non-zero charge density Q and magnetic field B along the $z-$axis. The metric ansatz is

$$ds^2=-U(r)dt^2+\frac{dr^2}{U(r)}+e^{2V(r)}(dx^2+dy^2)+e^{2W(r)}dz^2.$$

Maxwell's equations give

$$F=Qe^{-2V(r)-W(r)}dr\wedge dt+Bdx\wedge dy,$$

while Einstein's equations read

$$\begin{aligned} U\Big(V''-W''+\big(2V'+W'\big)\big(V'-W'\big)\Big)+U'\big(V'-W'\big) &= -2B^2e^{-4V} \\ 2V''+W''+2V'^2+W'^2 &= 0 \\ 3U''+3U'\big(2V'+W'\big) &= 24+4e^{-4V-2W}\big(B^2e^{2W}+2Q^2\big) \\ U'\big(2V'+W'\big)+2UV'\big(V'+2W'\big) &= 12-2e^{-4V-2W}\big(B^2e^{2W}+2Q^2\big). \end{aligned}$$

An analytic charged magnetic brane solution of this system eludes us, so we resorted to numerical integration.

We shoot from the horizon r_h to a UV cut-off r_c[1] where the space is AdS-like enough. The crucial point is that all (Q,B) solutions must agree asymptotically. In other words, we demand that at the UV cut-off r_c the values U_c, V_c and W_c match with those of the $Q=0, B=0$ pure AdS case. In this way our theories have the desired behaviour and the dual theories have the same unit-volume.
The boundary conditions are $U(r_h)=0$, $U'(r_h)=1$, $V(r_h)=V_h$, $W(r_h)=W_h$ and the rest derivatives are set by Einstein's equations. The second one sets $T=\frac{1}{4\pi}$ leaving Q and B free. Our adjustable parameters to achieve the above matching are r_h, W_h and V_h.

Smooth solutions were found for $B=0$ and $Q\leq 2.44\sim\sqrt{6}$. For Q in that range we also had $B<B_{cr}$. More specifically, B_{cr} is an increasing function of Q with $B_{cr}(0)=\sqrt{3}$. In addition, B_{cr} and Q_{cr} are negligibly increasing with T as expected. Resolution to this $\sqrt{3},\sqrt{6}$ "mystery" was given in [25] where extremal solutions are discussed[2].

Inspection of the solutions shows that asymptotically ($r\to\infty$)

$$U(r)=r^2,\ e^{2V(r)}=vr^2,\ e^{2W(r)}=wr^2,$$

with v and w functions of Q and B. Accepting asymptotically-AdS solutions induces the rescalings $\tilde{x}=\sqrt{v}x$, $\tilde{y}=\sqrt{v}y$ and $\tilde{z}=\sqrt{w}z$ and in turn sets the physical magnetic field of the boundary theory to[3]

$$\mathcal{B}_{\text{phys}}=\sqrt{3}\frac{B}{v},$$

[1] Our calculations turned out to be independent of how large r_c is.

[2] What actually happens is that on the parameter curve $Q^2+2B^2=6$ we have $U'(1)=0$ while we had assumed $U'(1)=1$. More specifically, we reach extremality on this curve with a near horizon Reissner-Nordstrom $AdS_2\times\mathbb{R}^3$ geometry for zero magnetic field, BTZ$\times\mathbb{R}^2$ for zero electric charge and a warped $AdS_3\times\mathbb{R}^2$ for the rest.

[3] The $\sqrt{3}$ factor is adopted from [24].

while the entropy density of the black hole to

$$\frac{S}{V} = \frac{1}{4G_5} \frac{e^{2V_h+W_h}}{v\sqrt{w}}.$$

What is more, since we are interested in investigating the dual $\mathcal{N} = 4$ SYM theory with fixed chemical potential μ (grand canonical ensemble), it turns out that the charge density Q is bound by the condition

$$Q = \frac{\mu}{\int_{r_h}^{r_c} e^{-2V(r)-W(r)} dr}. \tag{4.2}$$

For every B and fixed μ, Q is determined automatically. Therefore, when generating solutions, Q has to satisfy that relation to a sufficient accuracy. Playing this numerical game involved creating the final (μ, Q, B) black brane by taking small dQ, dB steps so that we not only prevent any "jump" and fail in the asymptotic matching but also filter out the right Q.
After consecutive days of a poor computer running we found the dependence $Q(B)\Big|_{\mu}$ for several chemical potentials. The results are shown in figure 4.1. Interested in the qualitative behaviour, we use dimensionless quantities.

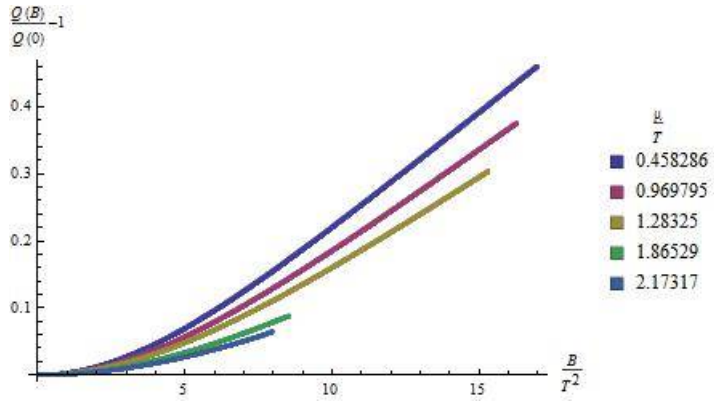

Figure 4.1: $\frac{Q(B)-Q(0)}{Q(0)}$ versus dimensionless magnetic field for different chemical potentials $\frac{\mu}{T}$.

We observe that for small B the dependence is quadratic and then evolves to a linear tail. In addition, the response of Q decreases with increasing μ. At the endpoints of the curves we stumble upon extremal solutions and further integration is impossible.

This calculation can be parallelised with what happens to the charge of a relativistic gas, [26]. In the grand canonical ensemble, the charge density is

$$\frac{Q}{V}=\frac{T}{V}\frac{d}{d\mu}\ln\mathcal{Z}=\frac{2|e|B}{(2\pi)^2\hbar c}\sum_n\int_0^{+\infty}dk\left(\frac{1}{e^{\beta(E_{n,k}-\mu)}+1}-\frac{1}{e^{\beta(E_{n,k}+\mu)}+1}\right), \tag{4.3}$$

where the sum is over the Landau levels for the particles and anti-particles.

Although relation (4.3) is, perturbatively speaking, out of reach for a super-Yang-Mills theory at strong coupling, our calculation in the dual theory should account for non-perturbative effects, such as the "magnetic dressing" of the propagators *à la* Schwinger, and is closely related to charge renormalization and the Debye length, [27].

With a set of constant-μ solutions at hand, we calculate the dimensionless entropy

$$\frac{S}{N_c^2V_3\mathcal{B}_{\rm phys}^{3/2}}=\frac{3^{-3/4}}{2\pi}\sqrt{\frac{v}{B^3w}}e^{2V_h+W_h}.$$

The results are the following.

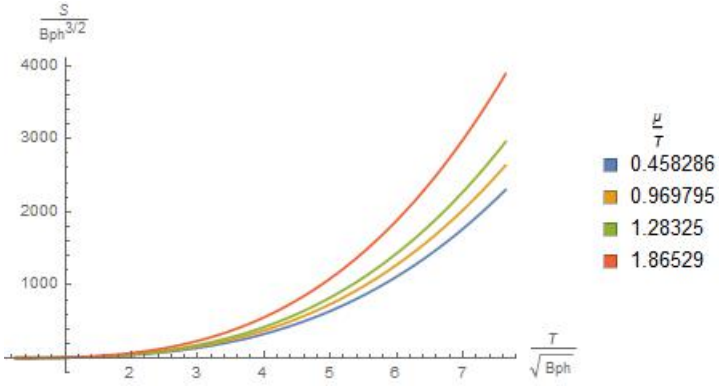

Figure 4.2: $\frac{S}{\mathcal{B}^{3/2}}$ versus $\frac{T}{\sqrt{\mathcal{B}}}$ for five chemical potentials.

The entropy is enhanced by the magnetic field as we also see on the lattice and decreased by the chemical potential, both effects not very clear from a field theory point of view.

The weak-strong B limits are important. For $T^2\gg B$, the system is conformal and the entropy scales as T^3 just as in $3+1$ $\mathcal{N}=4$ SYM. More interestingly, at strong magnetic field ($B\gg T^2$), the near-horizon geometry is BTZ $\times\,\mathbb{R}^2$ and the entropy scales as BT. The flow to this IR fixed point has a very elegant field theory interpretation.

In $3+1$ $\mathcal{N}=4$ SYM with a dominating magnetic field B, the wavefunctions

of the adjoint particles get quantized in a Landau sense. While they are all massless, the magnetic field gives dynamical mass $m^2 \sim B$ to everyone except for the zero-mode fermions, those with spin aligned with B. With increasing B, the motion of the particles gets more and more constrained along its direction and the low energy physics will be dominated by the massless zero-mode fermions. Therefore, in the large B limit, the system is effectively a $1+1$ CFT whose entropy for dimensional reasons will scale as $S \sim BT$.
So, we assert that this *dimensional reduction* is realised holographically by the near-horizon BTZ geometry in the gravity side.

4.2 Veneziano QCD

As explained earlier, the effects of flavoured quarks can be taken into account only in the Veneziano limit in which

$$N_c \to \infty,\ N_f \to \infty \text{ with } \chi = \frac{N_f}{N_c} \text{ and } \lambda = g_{\rm YM}^2 N_c \text{ fixed.}$$

A consistent extension of IHQCD in this limit is *Veneziano QCD* (V-QCD), [20].
Stacks of N_f space-filling $D4-\bar{D}4$ brane-antibrane pairs are embedded in spacetime and interact with the N_c color branes. The lowest modes of strings with both ends at the same (anti-)branes are the (left) right gauge fields $A^{L/R}$. These are dual to the spin-one quark bilinears

$$\bar{\psi}^i_{L/R}\sigma^\mu\psi^j_{L/R} \leftrightarrow A^{L/R\mu}_{ij}.$$

The lightest mode of $D-\bar{D}$ strings is a complex scalar matrix T_{ij} transforming in the bifundamental representation of flavor symmetry $U(N_f)_L \times U(N_f)_R$. It is called tachyon because its mass in the UV is negative $-\frac{3}{R^2}$. Its dual has conformal dimension $\Delta = 3$ and is identified with the chiral condensate

$$\bar{\psi}^i_R\psi^j_L \leftrightarrow T_{ij}.$$

Its existence proves vital because its divergence ($\tau \to \infty$) in the IR in confined geometries yields the physically correct regularity condition[4]. This tachyon condensation, synonymous to chiral condensation, is a necessary ingredient of the dynamics, [23].
In the vacuum state, $A^{L,R}$ can be set to zero and the Wess-Zumino term does

[4]Roughly speaking, with a diverging tachyon the branes "fuze" in the IR and the UV physics becomes independent of the IR.

not contribute to the thermodynamics. We consider $T(r) = \tau(r)\mathbb{I}_{N_f\times N_f} \in \mathbb{R}$ and also a $U(1)$ gauge field A_μ turned on to accommodate the magnetic field and the baryon density. The flavor action is (2.7) transformed to the Einstein frame,

$$S_f = -\chi M_P^3 N_c^2 \int d^5x V_f(\lambda,\tau)\sqrt{-\det\left(g_{\mu\nu} + w(\lambda)F_{\mu\nu} + k(\lambda)(\partial\tau)^2\right)}. \quad (4.4)$$

The full action $S = S_g + S_f$ is

$$S = M_P^3 N_c^2 \int d^5x\sqrt{-g}\Bigg(R - \frac{4}{3}\frac{\left(\partial\lambda\right)^2}{\lambda^2} + V_g(\lambda) - \chi V_f(\lambda,\tau)\sqrt{\det\left(\delta^\mu_\nu + w(\lambda)F^\mu_\nu + k(\lambda)\partial^\mu\tau\partial_\nu\tau\right)}\Bigg) + S_{\rm GH}. \quad (4.5)$$

The parameters are not rigorously determined from string theory but get constrained by physical requirements. First of all, the flavor potential V_f has to vanish exponentially as the tachyon condensates in the IR. So, we parametrize $V_f(\lambda,\tau) = V_{f0}(\lambda)e^{-a(\lambda)\tau^2}$. Second, the holographic beta function $\frac{d\lambda}{dA} \equiv \beta(\lambda,\tau)$ has to match the QCD $\beta-$function in the UV ($\lambda \to 0$, $\tau \to 0$). Up to two loops,

$$\beta^{\rm QCD}(g) = -\frac{g^3}{(4\pi)^2}\left[\frac{11}{3}N_c - \frac{2}{3}N_f\right] - \frac{g^5}{(4\pi)^4}\left[\frac{34}{3}N_c^2 - \frac{N_f}{N_c}\left(\frac{13}{3}N_c^2 - 1\right)\right],$$

and in terms of the 't Hooft constant λ,

$$\dot\lambda = -b_0\lambda^2 + b_1\lambda^3 + \mathcal{O}(\lambda^4) \quad (4.6)$$

where $b_0 = \frac{2}{3}\frac{11-2\chi}{(4\pi)^2}$, $\frac{b_1}{b_0^2} = -\frac{3}{2}\frac{34-13\chi}{(11-2\chi)^2}$.
What is more, $\bar\psi_L\psi_R$ has perturbative anomalous dimension

$$\gamma^{\rm QCD} \equiv -\frac{d\,\ln m}{d\,\ln\mu} = \frac{a_0}{4\pi}g^2 + \frac{a_1}{(4\pi)^2}g^4 + \dots \quad (4.7)$$

which at large N_c becomes

$$\gamma^{\rm QCD} \approx \frac{3}{(4\pi)^2}\lambda + \frac{203-10\chi}{12(4\pi)^4}\lambda^2 + \mathcal{O}(\lambda^3, N_c^{-2}). \quad (4.8)$$

We therefore require that $\beta(\lambda,\tau)$ and $\frac{d\tau}{dA} \equiv \gamma(\lambda,\tau)$ equate to (4.6) and (4.8) as $\lambda \to 0$. For this, exactly as in IHQCD, we assume regular expansions of (V_g, V_{f0}, k, w, a) around $\lambda = 0$ and extract constraints on them.
Another constraint comes from the IR ($\lambda \to \infty,\ \tau \to \infty$) where the potential needs to confine, setting $V_g \sim \lambda^{4/3}\sqrt{\ln\lambda}$, whereas the rest should keep the IR singularity "good".

A choice of potentials that fulfil the above and was used is the following:

- $V_g(\lambda) = \frac{12}{\ell}\left(1+V_0\lambda+V_1\lambda^{4/3}\sqrt{\log\left[1+V_2\lambda^{4/3}+V_3\lambda^2\right]}\right)$ (IHQCD model),
  $V_0 = \frac{11}{27\pi^2}, V_1 = 11000\frac{11^{1/3}}{81\pi^{8/3}}, V_2 = \frac{21335161\times 11^{-2/3}}{40144896000000\pi^{8/3}}$,
  $V_3 = \frac{12100000}{729\pi^4}, \ell = 1$
- $V_f(\lambda,\tau) = V_{f0}(\lambda)e^{-a_0\tau^2}, V_{f0}(\lambda) = W_0(1+W_1\lambda+W_2\lambda^2)$
  $a_0 = \frac{12-\chi W_0}{8}, W_0 = \frac{3}{11}, W_1 = \frac{24+W_0(11-2\chi)}{27\pi^2 W_0}$,
  $W_2 = \frac{24(857-45\chi)+W_0(4619-1714\chi+92\chi^2)}{46656\pi^4 W_0}$
- $k(\lambda) = \frac{\left(1+\ln\left[1+\frac{\lambda}{\lambda_0}\right]\right)^{-1/2}}{\left(1+\frac{1}{9}\left(\frac{203}{54}-\frac{16\chi}{27}\right)\frac{\lambda}{\lambda_0}\right)^{4/3}}$,
  $w(\lambda) = k(\lambda)$,
  $\lambda_0 = 8\pi^2$

This choice reproduces qualitatively the correct finite T QCD phase diagram and for $\chi \to 0$ one recovers the original fitted IHQCD results. We have fixed $\chi = 0.1$, small enough not to change the system since we are interested in the qualitative changes that small flavor induces.

4.2.1 The Background

To first approximation, we consider the flavor not backreacting to the glue. For this we will assume that the tachyon is negligible and set it to zero (chiral symmetric phase). Further, to be consistent, taking the field strength $F^2 \ll \mathcal{O}(1)$ we expand the square root up to the Maxwell term. Finally, we end up with an Einstein-Maxwell-Dilaton problem,

$$S = -\frac{1}{16\pi G_5}\int d^5x\sqrt{-g}\left(R - \frac{4}{3}\frac{\left(\partial\lambda\right)^2}{\lambda^2} + V_g(\lambda) - \chi V_f(\lambda,0) - Z(\lambda,0)F^2\right) + S_{\rm GH} \tag{4.9}$$

with $Z(\lambda,\tau) \equiv \frac{1}{4}V_f(\lambda,\tau)w^2(\lambda)$.
Interested in the deconfined phase[5], we are looking for black hole solutions. Our metric ansatz in conformal coordinates is

$$ds^2 = e^{2A(r)}\left(-f(r)dt^2 + \frac{dr^2}{f(r)} + dx^2 + dy^2 + e^{2W(r)}dz^2\right)$$

[5]Deconfinement in V-QCD is not in direct equivalence with chiral symmetry, [21]. Here we choose the purely chirally symmetric phase.

with $W(r)$ the factor breaking the full $SO(3)$ invariance to rotations around the z-axis due to the non-zero magnetic field.
The electromagnetic potential is taken

$$A_\mu = \Big(\mathcal{A}_0(r), Byh(r), 0, 0, 0\Big)$$

generating electric field $F_{tr} = \mathcal{A'}_0(r)$, magnetic field $F_{xy} = Bh(r)$ and a component $F_{rx} = Byh'(r)$. From the Maxwell equations $\nabla_\nu\Big(ZF^{\nu\mu}\Big) = 0$, for $\mu = x$ we get

$$e^{A(r)+W(r)} f(r) y h'(r) = const$$

For $y = 0$ we get $const = 0$ which implies $h'(r) = 0$ and the magnetic field is constant along the holographic direction generally. For $\mu = t$ we solve

$$\mathcal{A'}_0(r) = \frac{Qe^{-A(r)-W(r)}}{Z[\lambda(r)]},$$

which ultimately gives

$$\mathcal{A}_0(r) = \mu_b + Q\int_{-\infty}^{r} dv \frac{e^{-A(v)-W(v)}}{Z[\lambda(v)]}.$$

Fixing the gauge such that $\mathcal{A}_0(r_h) = \mu_h = 0$, the gauge field is non-singular at the horizon and the chemical potential is

$$\mu = \mu_b - \mu_h = \mu_b = \int_{-\infty}^{r_h} dr \mathcal{A'}_0(r). \tag{4.10}$$

Einstein's equations read

$$f'' + f'(3A' + W') = 4\chi \frac{Q^2 e^{-4A-2W}}{Z[\lambda]} + 4\chi B^2 Z[\lambda] e^{-2A}, \tag{4.11}$$

$$(fW')' + fW'(3A' + W') = 2\chi B^2 Z[\lambda] e^{-2A}, \tag{4.12}$$

$$3A'' + W'' = 3A'^2 - W'^2 - \frac{4}{3}\frac{\lambda'^2}{\lambda^2}, \tag{4.13}$$

$$\begin{aligned} 12f(A')^2 + 3f'A' + f'W' + 6fA'W' = {} & \frac{4}{3} f \frac{\lambda'^2}{\lambda^2} + e^{2A} V_d(\lambda) - 2\chi \frac{Q^2 e^{-4A-2W}}{Z[\lambda]} \\ & - 2\chi B^2 Z[\lambda] e^{-2A} \end{aligned} \tag{4.14}$$

with the "flavor-modified" dilaton potential $V_d(\lambda) \equiv V_g(\lambda) - \chi V_f(\lambda, 0)$. The equation of motion of the dilaton

$$f\left(\frac{\lambda''}{\lambda} - \left(\frac{\lambda'}{\lambda}\right)^2\right) + \frac{\lambda'}{\lambda}\Big(f' + f(3A' + W')\Big) = -\frac{3}{8} e^{2A} \lambda (\partial_\lambda V_d) + \frac{3}{4}\chi\lambda(\partial_\lambda Z)\left(B^2 e^{-2A} - \frac{Q^2 e^{-4A-2W}}{Z[\lambda]^2}\right) \tag{4.15}$$

is automatically satisfied from differentiating the constraint equation 4.14, so the system is first-order in λ.

A convenient trick for easier integration of the system is to use the scale factor A as coordinate instead of r, defined as $\frac{dr}{dA} = q(A)e^{-A}$. The resulting equations are presented in Appendix B. The entire numerical analysis was done in Mathematica and is described in Appendix C.

4.2.2 Thermodynamics

With the generated solutions we can study the thermodynamics for varying Q and B. Recall that he have set $\chi = 1/10$.

Phase Structure

The plot of the (dimensionless) $T(\lambda_h)$ relation in figure 4.3 reveals the phase structure of the system. Obviously, it does not differ much from the IHQCD counterpart because χ is small.

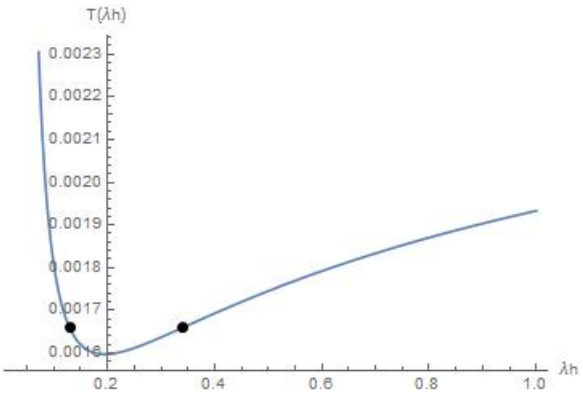

Figure 4.3: Plot of T versus λ_h for our model for $Q = B = 0$. The decreasing leg corresponds to stable big black holes and the increasing one to unstable small ones. The black bullet denotes the dimensionless $T_c = 0.001659$.

Furthermore, we can see how the magnetic field changes the Hawking-Page transition. In a confining background with $B = 0$ the string "rests" at A^*, the minimum of $A_s(A) = A + \frac{2}{3}\phi(A)$. Turning on B along the direction of the quarks contributes a factor $\frac{W(A)}{2}$ to A_s (Appendix A) and the minimum displaces with changing B. A deconfinement phase transition occurs when the horizon of a growing black hole passes A^*. So the change of A^* with B is an indicator of this transition.
We approximate the thermal gas phase by working deep in the small

black hole branch[6], here $\lambda_h = 100$. We found that A^* approaches the boundary as B increasing, implying an increasing T_c.

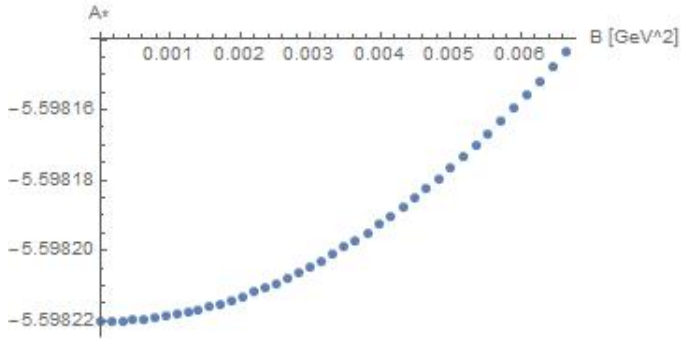

Figure 4.4: The minimum of A_s versus the magnetic field B.

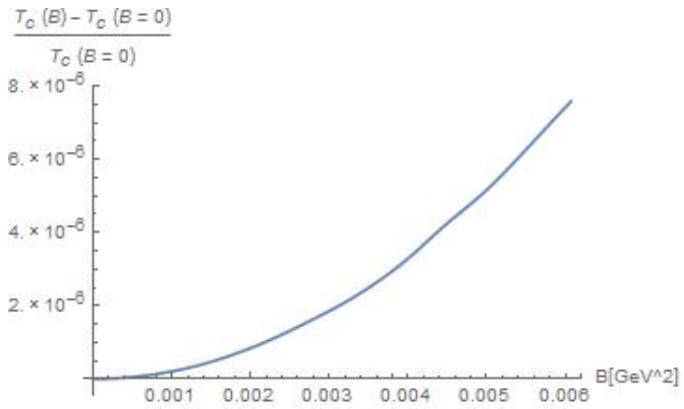

Figure 4.5: T_c versus B.

This behaviour is in disagreement with the lattice results (figure 1.7). One has to remark that this calculation is heuristic because no free energy differences were involved and the quarks were treated as probes. Nevertheless it should give a hint for the general behaviour of $T_c(B)$. As a side note, in the top-down $D3/D7$ model it is found that T_c increases with B, [28].

Free Energy

The free energy is the on-shell action. Plugging the contracted Einstein

[6]Roughly speaking, as $\lambda_h \to \infty$ the horizon shrinks and $T \to 0$ (thermal gas). This is justified in [17].

equation

$$R = \frac{4}{3}\big(\partial\phi\big)^2 + \frac{1}{3}Z(\lambda)F^2 - \frac{5}{3}V_d(\lambda)$$

into (4.9),

$$S_{\text{on-shell}} = \frac{1}{24\pi G_5}\int d^5x\sqrt{-g}\Big(V_d(\lambda) + Z(\lambda)F^2\Big) \tag{4.16}$$

Combining the equations of motions we find that

$$\sqrt{-g}V_d = -\Big[\Big(2W' + 3A'\Big)fe^{3A+W} - 2Q\mathcal{A}_0\Big]'$$

which reduces (4.16) to

$$\begin{aligned} S_{\text{on-shell}} &= \frac{1}{8\pi G_5}\int_0^\beta dt\int d^3x\int_0^{r_h} dr\Big(\big(A' + W'\big)fe^{3A+W}\Big)' \\ &= -\frac{\beta V_3}{8\pi G_5}(A' + W')fe^{3A+W}\Big|_{r\to 0}, \end{aligned} \tag{4.17}$$

with $\beta = \frac{1}{T}$ and V_3 the planar 3-volume.
The additional Gibbons-Hawking term is

$$S_{\text{GH}} = \frac{1}{8\pi G_5}\int_{\partial\mathcal{M}} d^4x\sqrt{-h}K.$$

In conformal coordinates, one obtains

$$\sqrt{-h} = e^{3A+W}\sqrt{f}\ ,\ K = \frac{f'}{2\sqrt{f}} + (4A' + W')\sqrt{f}$$

and S_{GH} becomes

$$S_{\text{GH}} = \frac{\beta V_3}{8\pi G_5}e^{3A+W}\left(\frac{f'}{2} + f(A' + W')\right)\Big|_{r\to 0}.$$

The total on-shell action is

$$\begin{aligned} S^{\text{TOTAL}}_{\text{on-shell}} &= \frac{\beta V_3}{8\pi G_5}e^{3A(r)+W(r)}\left(\frac{f'(r)}{2} + 3A'(r)f(r)\right)\Big|_{r\to 0} \\ &= \frac{\beta V_3}{8\pi G_5}\frac{e^{4A+W(A)}}{q(A)}\left(\frac{\dot{f}(A)}{2} + 3f(A)\right)\Big|_{A\to\infty}. \end{aligned} \tag{4.18}$$

Finally, the associated regularized free energy density is

$$F(T,Q,B) \equiv \frac{\mathcal{F}}{M_p^3 N_c^2 V_3} = \frac{e^{4A+W(A)}}{q(A)}\left(\frac{\dot{f}(A)}{2}+3f(A)\right)\Big|_{A\to A_{s0}}.$$

Only energy differences make sense and should be independent of the cut-off A_{s0}. However, this is not the case here since, according to [29], in the above formula there is a hidden logarithmic UV divergence of the type

$$I_{\log} = \frac{1}{64\pi G_5}\ln\epsilon \int d^4x\sqrt{\gamma^0}(F^0)^2,$$

where γ^0, F^0 are the regular induced metric and gauge field on the boundary. Numerically, disentangling these divergences was quite difficult to achieve . In order to have results as much as possible independent of the cut-off we computed the ratio $\frac{\mathcal{F}(T,\mu,B)-2\mathcal{F}(T,\mu,0)-\mathcal{F}(T,0,0)}{\mathcal{F}(T,\mu,0)-\mathcal{F}(T,0,0)}$. By reinserting dimensions through the string length $\ell_s^{-1} = 98890$ MeV we get the following plot for B up to the maximum value studied on the lattice and for μ in different corners of the phase diagram .

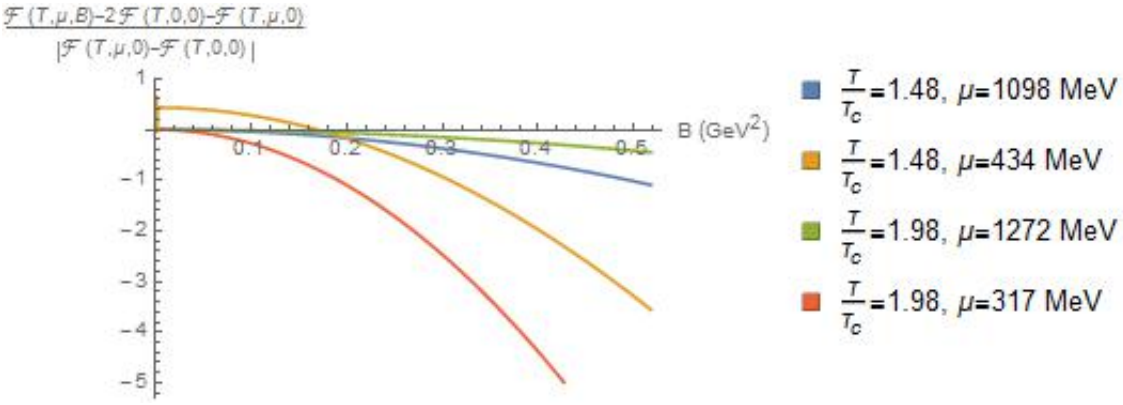

Figure 4.6: Rescaled free energy versus magnetic field for four different states (T,μ). $T_c \equiv T_c(\mu=0,B=0) = 155$ MeV.

The plot is still infected with the cut-off-dependence but it presents a consistent qualitative behaviour and that is the magnetic field decreases the free energy, makes the black hole more stable. This could point to a decreasing T_c and inverse magnetic catalysis of the chiral condensate. One though needs to properly subtract the thermal gas and black hole entropies to see what is really happening.

Entropy

The entropy density is

$$\frac{S}{M_p^3 N_c^2 V_3} = \frac{\mathcal{A}_h}{4} = \frac{e^{3A_h + W(A_h)}}{4}. \tag{4.19}$$

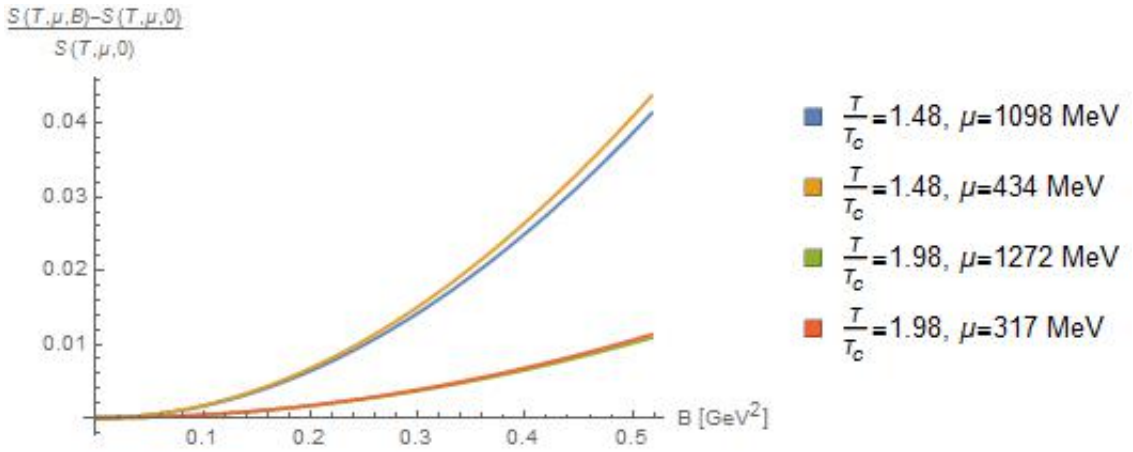

Figure 4.7: Rescaled entropies for four different states (T, μ).

The major result is that again the entropy gets enhanced by the magnetic field almost quadratically. This dependence was expected though because only χB^2 terms appear in the system and they are numerically small. It is also obvious that increasing the chemical potential the entropy falls a bit.

Charge Density

As in the Kraus D'Hoker model, we also calculated the response of the electric charge density Q to the magnetic field B. The results are similar with the charge increasing with B.

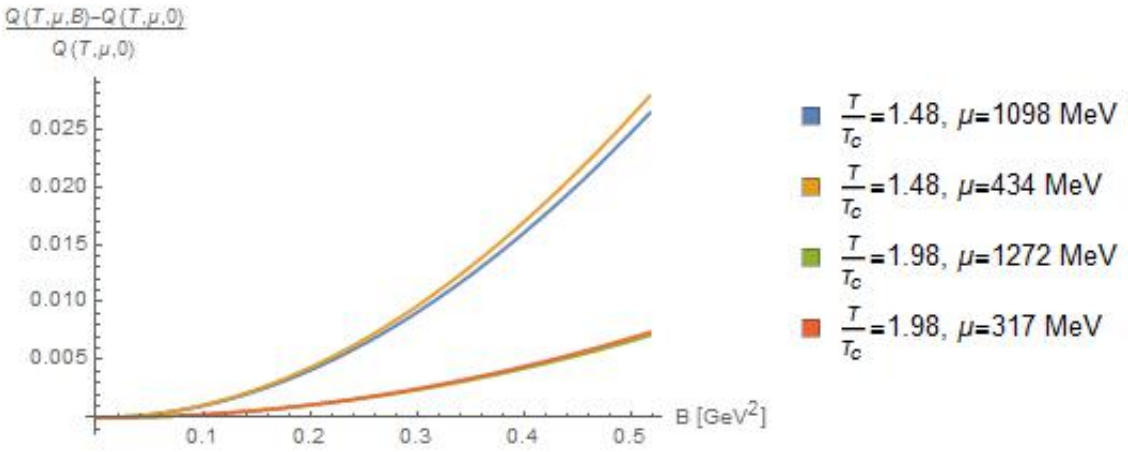

Figure 4.8: Rescaled entropies for four different states (T, μ).

Discussion and Outlook

Our findings in the Kraus D'Hoker model show that strong magnetic field does have an impact on the physics. In specific, the IR geometry reveals a holographic realization of the dimensional reduction due to a strong magnetic field. In the V-QCD model, the results should be judged on the basis of our assumptions: zero tachyon field, small Q and B and $\chi = 1/10$. Hence, we do not expect significant changes in the vacuum solutions from IHQCD. Our indirect calculation of an increasing T_c with B is heuristic and, in principle, is done by subtracting thermal gas and black hole free energies. Their expressions give many numerical errors but there is a better way to do that, independent of the UV cut-off. Using the 1^{st} law of thermodynamics, at constant chemical potential the free energy is

$$\mathcal{F}(T) = \mathcal{F}_o - \int_{T_o}^{T} S dT = -\int_{\infty}^{\lambda_h(T)} S(\tilde{\lambda}_h) T'(\tilde{\lambda}_h) d\tilde{\lambda}_h.$$

This integral representation is more precise numerically but it assumes the knowledge of the full $T(\lambda_h)$ diagram, which makes it also not so time-efficient.

As for the future, there are plenty of extensions to be considered. First of all, a systematic study of the thermal gas background is necessary for consistent investigation of the deconfining phase transition. This would require the search of the appropriate "good" IR behaviour for the metric. Second, a more realistic treatment of the flavors in V-QCD would take into account the tachyon and its backreaction to the geometry. The changes will be dramatic since the tachyon always diverges in the IR in the confined phase. Physical requirements on its IR behaviour constrain further the potentials used. In addition, a tower of tachyon solutions with the same quark mass (non-renormalizable mode) and arbitrary nodes is well expected to appear. From this degeneracy of the so-called Efimov Vacua only the zero-node solution has the smallest energy and should be selected. The fruit of all this added complexity is new intermediate black hole phases even with non-vanishing chiral condensate, [22], that change the thermodynamics. Of course this also open the path for magnetic effects on chiral symmetry breaking and color

superconductivity. One possible scenario is that the magnetic field coupled to the condensate makes the chirally broken deconfined phase disappear, i.e. magnetic decatalysis. Another question worth asking is how the (T, μ, B) phase diagram changes as a function of χ and how the glueball and mesonic spectra are affected by B.

From a practical point of view, it is also remarkable that studying the full system is a very demanding numerical task and an automated code for matching Q with μ and B as well as a supercomputer would come handy. Ultimately, the findings should be fitted with lattice data in the Veneziano limit that unfortunately are not available to date.

Acknowledgements

First, I would like to thank Umut for his continuous support and enthusiasm in this project as well as his guidance during this last year of my master studies. Second, I would like to thank my classmate and friend Jorgos Papadomanolakis with whom I enjoyed collaborating throughout this journey. This work should be considered as a team venture including endless hours of discussions in and out of physics. Thanks also to Tara, Olga, Panos and Aron for the useful discussions and to Ioannis Iatrakis and Matti Järvinen for last-minute research advice. Hail to Lambros for our transatlantic tense talks and him helping me this year. I shouldn't leave out my fellow classmates and people I connected with in Utrecht and made me feel at home and were a positive influence to me. I will miss you but I'm sure we will meet sooner or later. Special thanks to my buddies in Greece who took a big part in those two years in their own way. Last but not least, I am grateful for my family believing in me in every step I take.

Appendices

The Wilson-Loop Test

Holographically, the Wilson loop is computed as the exponential of minus the minimum area of the string worldsheet.
Let a quark and an antiquark at distance L on the z-direction, evolving in time T and $E(L)$ their potential energy. The holographic statement, in the string frame, is

$$TE(L) = S_{\text{Nambu-Goto}}[X^\mu_{\text{min}}(\sigma,\tau)] = T_f \int d\sigma d\tau \sqrt{-\det g_s}, \tag{4.20}$$

where X^μ_{min} is the string configuration that sweeps the minimum worldsheet area and $(g_s)_{ab} = (g_s)_{\mu\nu}\partial_a X^\mu \partial_b X^\nu$ the induced metric on it. For a general metric with $SO(2)$ symmetry due to the magnetic field along the z-direction

$$ds^2 = -g_{00}dt^2 + g_{\perp\perp}\Big(dx^2 + dy^2\Big) + g_{|||}dz^2 + g_{rr}dr^2$$

and choosing the gauge $\tau = t$, $\sigma = z$ and $X^\mu = \begin{pmatrix} t \\ 0 \\ 0 \\ z \\ r(z) \end{pmatrix}$, the Nambu-Goto action reads

$$S_{\text{NG}} = T_f T \int dz \sqrt{g_{00}g_{|||} + g_{00}g_{rr}r'^2} = T_f T \int dz \sqrt{f^2(z) + g^2(z)r'^2}$$

having defined $f^2(z) \equiv g_{00}g_{|||}$, $g^2(z) \equiv g_{00}g_{rr}$. The system can be regarded as a one-dimensional lagrangian system with $\mathcal{L} = \sqrt{f^2(z) + g^2(z)r'^2}$. The hamiltonian is

$$H = p_r r' - \mathcal{L} = \frac{\partial \mathcal{L}}{\partial r'} r' - \mathcal{L} = \frac{g^2(z)r'^2}{\sqrt{f^2(z) + g^2(z)r'^2}} - \sqrt{f^2(z) + g^2(z)r'^2} = -\frac{f^2(z)}{\mathcal{L}(z)}.$$

The system is σ-independent, thus H is conserved.
Let $z = 0$ be the turning point where $r'(z = 0) = 0$ and the string turns having probed up to r_0 in the bulk. Then,

$$H = -\frac{f^2(z=0)}{\mathcal{L}(z=0)} = -f(z=0) \implies \mathcal{L}_{\text{on-shell}} = \frac{f^2(z)}{f(z=0)}. \tag{4.21}$$

The distance between the quark and the antiquark is

$$L = \int_{-\frac{L}{2}}^{\frac{L}{2}} dz = \int \frac{dz}{dr} dr = \int \frac{dr}{r'} = 2\int_{r_B}^{r_o} \frac{dr}{r'} \overset{(4.21)}{=} 2\int_{r_B}^{r_o} dr \frac{g(r)}{f(r)} \frac{1}{\sqrt{f^2(r)/f^2(r_o) - 1}}, \tag{4.22}$$

where $r_B = 0$ denotes the brane and the factor of two comes from the symmetry of the shape $r(z)$ with respect to r_o. The quark-antiquark potential (4.20) now reads

$$\begin{aligned} E(L) = \int \mathcal{L}_{\text{on-shell}} dz &= \int dr \frac{1}{r'} \frac{f^2(r)}{f(r_o)} = 2\int_0^{r_o} dr \frac{g(r)}{f(r)} \frac{f^2(r)}{\sqrt{f^2(r) - f^2(r_o)}} \\ &= T_f f(r_o) L + 2T_f \int_0^{r_o} dr \frac{g(r)}{f(r)} \sqrt{f^2(r) - f^2(r_o)}. \end{aligned} \tag{4.23}$$

The expression diverges and needs regularization by substracting the quark masses. However, confinement is independent of that. When the quark and antiquark are confined then the first term in (4.23) dominates and one retrieves a linear potential.
By simple inspection, the second term is always finite. On the other hand, in the string frame where $ds^2 = e^{2A(r)+\frac{4}{3}\phi(r)}(-dt^2 + dr^2 + dx^2 + dy^2 + e^{2W(r)}dz^2)$, the first term reads

$$L = 2\int_0^{r_o} dr \sqrt{\frac{g_{rr}(r)}{g_{|||}(r)}} \frac{1}{\sqrt{\frac{g_{00}(r)g_{|||}(r)}{g_{00}(r_o)g_{|||}(r_o)} - 1}} = 2\int_0^{r_o} dr \frac{e^{-W(r)}}{\sqrt{e^{4A_s(r)-4A_s(r_o)} - 1}},$$

with $A_s(r) = A(r) + \frac{W(r)}{2} + \frac{2}{3}\phi(r)$.
This is finite near the boundary $r = 0$ because $e^{-2A_s} \sim r^2$. Expanding the integrand around the turning point r_o,

$$\frac{1}{\sqrt{e^{4A_s(r)-4A_s(r_o)} - 1}} \approx \frac{1}{\sqrt{4A_s'(r_o)(r - r_o) + 2A_s''(r_o)(r - r_o)^2 + \dots}},$$

one observes that its integral is always finite unless r_o coincides with a minimum of A_s, r^* where $A_s'(r^*) = 0$. Therefore, as r_o approaches r^*, $E(L) \sim T_f e^{2A_s(r^*)} L$ exhibiting confinement. As a result, the requirement for confinement in the IR translates to finding which dilaton potentials create a minimum for A_s.
This derivation is based on [18].

The A-coordinate System

Switching from the r to A coordinates with the transformation

$$\frac{dr}{dA} = q(A)e^{-A},\ r(A=+\infty) = 0,$$

the equations of motion for the gravitational background read:

$$\begin{aligned}
\ddot{f} + \dot{f}\left(4 + \dot{W} - \frac{\dot{q}}{q}\right) &= q^2\left(4\chi\frac{Q^2e^{-6A-2W}}{Z(\lambda)} + 4\chi B^2 Z(\lambda)e^{-4A}\right),\\
f\ddot{W} + \dot{W}\left(\dot{f} + f\left(4 + \dot{W} - \frac{\dot{q}}{q}\right)\right) &= 2\chi B^2 q^2 Z[\lambda]e^{-4a},\\
\ddot{W} + \dot{W}\left(1 + \dot{W} - \frac{\dot{q}}{q}\right) + \frac{4}{3}\frac{\dot{\lambda}^2}{\lambda^2} &= 3\frac{\dot{q}}{q},\\
12f + 3\dot{f} + \dot{f}\dot{W} + 6f\dot{W} &= \frac{4}{3}f\frac{\dot{\lambda}^2}{\lambda^2} + q^2V_d(\lambda) - 2\chi Q^2\frac{q^2e^{-6A-2W}}{Z(\lambda)}\\
&\quad - 2\chi B^2q^2Z(\lambda)e^{-4A},
\end{aligned}$$

where the dot $\dot{}$ denotes derivative with respect to A.
Also the chemical potential 4.10 is

$$\mu = Q\int_{+\infty}^{A_h}\frac{q(A)e^{-2A-W(A)}}{Z[\lambda(A)]}\mathrm{d}A.$$

Numerical Method

The black hole solutions are found by shooting from the horizon A_h. Since integration is not possible at exactly the horizon because $f(A_h) = 0$, we shoot from $A_h + \epsilon$ with $\epsilon \ll 1$, e.g. $\epsilon = 10^{-8}$. Expanding around the horizon the initial values are:

$$\begin{aligned}
f(A_h+\epsilon) &= \epsilon\dot{f}(A_h) + \mathcal{O}(\epsilon^2)\\
\dot{f}(A_h+\epsilon) &= \dot{f}(A_h) + \epsilon\ddot{f}(A_h) + \mathcal{O}(\epsilon^2)\\
q(A_h+\epsilon) &= q_h + \epsilon\dot{q}(A_h) + \mathcal{O}(\epsilon^2)\\
W(A_h+\epsilon) &= W_h + \epsilon\dot{W}(A_h) + \mathcal{O}(\epsilon^2)\\
\dot{W}(A_h+\epsilon) &= \dot{W}(A_h) + \epsilon\ddot{W}(A_h) + \mathcal{O}(\epsilon^2)\\
\lambda(A_h+\epsilon) &= \lambda_h + \epsilon\dot{\lambda}(A_h) + \mathcal{O}(\epsilon^2)
\end{aligned}$$

By inserting $f(A_h) = 0$ in the Einstein and dilaton equations one can solve for q_h, $\dot{q}(A_h)$, $\ddot{f}(A_h)$, $\dot{W}(A_h)$, $\ddot{W}(A_h)$ and $\dot{\lambda}(A_h)$ as a function of λ_h, A_h, W_h and temperature $T = -\frac{f'(A_h)}{4\pi} = -\frac{e^{A_h}}{4\pi q(A_h)}\dot{f}(A_h)$.
We can give set $\dot{f}(A_h) = 1$ without loss of generality. The system of equations is solved by an NDSolve function which gets as input $(\lambda_h, A_h, W_h, Q, B)$. Solutions are found in the interval $[A_h+\epsilon, A_{\max}]$. Yet, there are still symmetry transformations of the equations we can utilize to refine the solutions.

Firstly, we demand all solutions to be asymptotically AdS. That means that as $A \to A_{\max}$, $f \to 1$. Thus, we rescale

$$\tilde{f}(A) = \frac{f(A)}{\delta f^2},\ \tilde{q}(A) = \frac{q(A)}{\delta f},$$

where $\delta f^2 = f(A_{\max})$.

Secondly, The z unit-length is normalized to zero by shifting

$$\tilde{W}(A) = W(A) - \delta W,\ \delta W = W(A_{\max}).$$

Last but not least, we demand that all solutions share the same UV asymptotics so that the dual theories are comparable. Since fixing the $\Lambda_{\rm QCD}$ integration constant is difficult numerically, we would rather set all solutions to have the same unknown $\Lambda_{\rm QCD}$. In other words, we want all dilatons to have the same value λ_{s0} at a specific point A_{s0} in the UV[7]. We achieve this by finding the point $A_{\rm eq}$ each dilaton acquires the value λ_{s0} and then shift the coordinate A

$$\tilde{A} = A - \delta A \text{ with } \delta A = A_{\rm eq} - A_{s0}.$$

In the end, the solutions meet all requirements and the physical quantities have been rescaled to keep the equations invariant:

$$\begin{aligned} T_{\rm new} &= -\frac{e^{\tilde{A}_h}\dot{\tilde{f}}(\tilde{A}_h)}{4\pi\tilde{q}(\tilde{A}_h)}, \\ Q_{\rm new} &= Qe^{-3\delta A-\delta W}, \\ B_{\rm new} &= Be^{-2\delta A}. \end{aligned}$$

From all these transformations, the dilaton remains intact, $\lambda(A) = \tilde{\lambda}(\tilde{A})$. The final solutions $\left(\tilde{q}(\tilde{A}),\ \tilde{f}(\tilde{A}),\ \tilde{W}(\tilde{A}),\ \tilde{\lambda}(\tilde{A})\right)$ are characterized by $\left(T_{\rm new},\ Q_{\rm new},\ B_{\rm new}\right)$.

[7]We used $\lambda_{s0} = 0.0099395755$ and $A_{s0} = 35.3461993045$.

Bibliography

[1] M. E. Peskin, D. V. Schroeder, *"An Introduction to Quantum Field Theory"*, Addison-Wesley, Reading, 1995

[2] F. Karsch, *"Lattice QCD at high temperature and density"*, Lect. Notes Phys. **583** (2002) 209-249, arXiv:hep-lat/0106019v2

[3] G. Boyd et al., *"Thermodynamics of SU(3) Lattice Gauge Theory"*, Nucl.Phys. **B469** (1996) 419-444, arXiv:hep-lat/9602007v1

[4] M. Panero, *"Thermodynamics of the QCD plasma and the large-N limit"*, Phys.Rev.Lett. **103** (2009), arXiv:0907.3719v2 [hep-lat]

[5] G. S. Bali, F. Bruckmann, M. Constantinou, M. Costa, G. Endrődi, Z. Fodor, S. D. Katz, S. Krieg, H. Panagoloupos, A. Schäfer, K. Szabó, *"Thermodynamic properties of QCD in external magnetic fields"*, (2013), arXiv:1301.5826v1 [hep-lat],
G. S. Bali, F. Bruckmann, G. Endrődi, S. D. Katz, A. Schäfer, *"The QCD equation of state in background magnetic fields"*, (2014), arXiv:1406.0269v1 [hep-lat]

[6] G. S. Bali, F. Bruckmann, G. Endrődi, Z. Fodor, S. D. Katz, A. Schäfer, *"QCD quark condensate in external magnetic fields"*, Phys. Rev. D **86** (2012), arXiv:1206.4205 [hep-lat]

[7] J. Maldacena, *"The Large N Limit of Superconformal Field Theories and Supergravity"*, Adv. Theor. Math. Phys. 2:231-252 (1998), arXiv:hep-th/9711200v3

[8] J. Casalderrey-Solana, H. Liu, D. Mateos, K. Rajagopal, U. A. Wiedemann, *"Gauge/String Duality, Hot QCD and Heavy Ion Collisions"*, (2012), arXiv:1101.0618v2 [hep-th]

[9] A. Karch, E. Katz, *"Adding flavor to AdS/CFT"*, JHEP **0206** (2002) 043, arXiv:hep-th/0205236v2

[10] E. Witten, *"Anti-de Sitter Space, Thermal Phase Transition, And Confinement In Gauge Theories"*, Adv. Theor. Math. Phys. 2:505-532 (1998), arXiv:hep-th/9803131

[11] T. Sakai, S. Sugimoto, *"Low energy hadron physics in holographic QCD"*, Prog.Theor.Phys.**113** (2005) 843-882, arXiv:hep-th/0412141v5

[12] M. Kruczenski, D. Mateos, R. C. Myers, D. J. Winters, *"Towards a holographic dual of large-N_c QCD"*, JHEP **0405** (2004) 041, arXiv:hep-th/0311270v4

[13] F. Preis, A. Rebhan, A. Schmitt, *"Inverse magnetic catalysis in dense holographic matter"*, JHEP **1103** (2011) 033, arXiv:1012.4785v3 [hep-th]

[14] J. Elrich, E. Katz, D. T. Son, M. A. Stephanov, *"QCD and a Holographic Model of Hadrons"*, Phys. Rev. Lett. **95** (2005), arXiv:hep-ph/0501128v2

[15] C. P. Herzog, *"A Holographic Prediction of the Deconfinement Temperature"*, Phys. Rev. Lett. **98** (2007), arXiv:hep-th/0608151v3

[16] U. Gürsoy, E. Kiritsis, *"Exploring improved holographic theories for QCD: Part I"*, JHEP **0802** (2008) 032 , arXiv:0707.1324v3 [hep-th],
U. Gürsoy, E. Kiritsis, F. Nitti *"Exploring improved holographic theories for QCD: Part II"*, JHEP **0802** (2008) 019, arXiv:0707.1349v3 [hep-th]

[17] U. Gürsoy, E. Kiritsis, L. Mazzanti, F. Nitti, *"Holography and Thermodynamics of 5D Dilaton-gravity"*, JHEP **0905** (2009) 033, arXiv:0812.0792v2 [hep-th]

[18] Y. Kinar, E. Schreiber, J. Sonnenschein, *"$Q\bar{Q}$ Potential from Strings in Curved Spacetime - Classical Results"*, Nucl.Phys. **B566** (2000) 103-125, arXiv:9811192v1 [hep-th]

[19] U. Gürsoy, E. Kiritsis, L. Mazzanti, F. Nitti, *"Improved Holographic Yang-Mills at Finite Temperature: Comparison with Data"*, Nucl.Phys. **B820** (2010) 148-177, arXiv:0903.2859v3 [hep-th]

[20] M. Järvinen, E. Kiritsis, *"Holographic Models for QCD in the Veneziano Limit"*, JHEP **1203** (2012) 002, arXiv:1112.1261v2 [hep-ph]

[21] T. Alho, M. Järvinen, E. Kiritsis, K. Tuominen, *"On finite-temperature holographic QCD in the Veneziano Limit"*, (2012), arXiv:1210.4516v1 [hep-ph]

[22] T. Alho, M. Järvinen, K. Kajantie, E. Kiritsis, C. Rosen, K. Tuominen, *"A holographic model for QCD in the Veneziano limit at finite temperature and density"*, (2013), arXiv:1312.5199v1 [hep-ph]

[23] R. Casero, E. Kiritsis, Á. Paredes, *"Chiral symmetry breaking as open string tachyon condensation"*, Nucl.Phys.**B787** (2007) 98-134, arXiv:0702155v1[hep-th]

[24] E. D'Hoker, P. Kraus, *"Magnetic Brane Solutions in AdS"*, JHEP **0910** (2009) 088, arXiv:0908.3875v3 [hep-th]

[25] E. D'Hoker, P. Kraus, *"Charged Magnetic Brane Solutions in AdS_5 and the fate of the third law of thermodynamics"*, (2009), arXiv:0911.4518v2 [hep-th]

[26] D. E. Miller, P. S. Ray, *"Thermodynamics of a Relativistic Fermi Gas in a Strong Magnetic Field"*, Helv.Phys.Acta **57** (1985) 96 BI-TP 82/27, IAEA RN:15042391

[27] A. Gorsky, P. N. Kopnin, A. Krikun, *"Anomalous QCD Contributions to the Deybe Screening in an External Field via Holography"*, Phys. Rev. D **83** (2011), arXiv:1012.1478v2 [hep-ph]

[28] O. Bergman, J. Erdmenger, G. Lifschytz, *"A Review of Magnetic Phenomena in Probe-Brane Holographic Matter"*, (2012), arXiv:1207.5953v2 [hep-th]

[29] M. Taylor-Robinson, *"More on counterterms in the gravitational action and anomalies"*, arXiv:0002125v2 [hep-th]